JOURNAL OF PLANKTON RESEARCH | VOLUME 25 | NUMBER 1 | PAGES 35–61 | 2003

Phytoplankton spectral absorption as influenced by community size structure and pigment composition

STEVEN E. LOHRENZ[1]*, ALAN D. WEIDEMANN[2] AND MERRITT TUEL[1]

[1]DEPARTMENT OF MARINE SCIENCE, THE UNIVERSITY OF SOUTHERN MISSISSIPPI, 1020 BALCH BOULEVARD, STENNIS SPACE CENTER, AND [2]NAVAL RESEARCH LABORATORY, BUILDING 1009, STENNIS SPACE CENTER, MS 39529–0001, USA

*CORRESPONDING AUTHOR: Steven.Lohrenz@usm.edu

Assessments were made of the relative importance of package effects and pigment composition in contributing to variations in spectral absorption in shelf waters off North Carolina during May 1997 and off west Florida during October 1998. Measurements of spectral absorption of size-fractionated particulate material on glass fibre filters were made using two methods, the transmittance–reflectance (T–R) method and the quantitative filter technique (QFT). Spectral absorption of phytoplankton pigments was decomposed into a series of 13 Gaussian absorption bands, and absorption band peak heights were related to concentrations of major pigment classes. Maximum weight-specific pigment absorption coefficients for individual absorption bands (p^*_m) derived from the fit of a hyperbolic tangent function to the data were found to be similar for North Carolina and west Florida shelf waters. The values were used to reconstruct spectral absorption in the absence of pigment packaging, which was then compared to measured absorption to provide an assessment of pigment packaging. Package effects were found to be responsible for up to a 62% reduction in the amplitude of major absorption bands, particularly for samples from low-salinity waters and for populations dominated by larger (>3 μm) phytoplankton. Variations in pigment composition were also found to have an impact, although it was smaller (10–28%), on variations in total absorption. Potential bio-optical applications of the Gaussian decomposition approach include the estimation of pigment concentrations from in situ or remotely sensed ocean colour observations. Alternatively, where pigment concentrations are known, it may be possible to estimate absorption. Successful application of such techniques may necessitate characterizations of coefficients specific to a given region and time.

INTRODUCTION

Phytoplankton light absorption is a major factor contributing to the variation in optical properties of oceanic and coastal waters. The properties of phytoplankton spectral absorption form an integral part of a variety of bio-optical algorithms to estimate phytoplankton biomass and other constituents (Roesler and Perry, 1995; Garver and Siegel, 1997; Bricaud *et al.*, 1998; He *et al.*, 2000; Sathyendranath *et al.*, 2001) and model primary production (Platt and Sathyendranath, 1988; Morel, 1991; Sosik, 1996; Bouman *et al.*, 2000a,b; Lohrenz *et al.*, 2002). Continued improvements in the performance and spectral resolution of *in situ* optical instruments and airborne and satellite sensors have generated increasingly sophisticated information about the optical properties of natural waters. Derivations of meaningful bio-optical information from these data hinge on improved understanding of the variability in absorption characteristics of phytoplankton and its relationship to phytoplankton community composition, size structure, and pigment concentrations.

Phytoplankton spectral absorption can vary as a consequence of composition and concentration of pigments as well as of pigment packaging (Duysens, 1956; Sathyendranath *et al.*, 1987; Hoepffner and Sathyendranath, 1991, 1993; Nelson *et al.*, 1993) and macromolecular interactions (Geider and Osborne, 1987; Kirk, 1994). Such factors are known to differ among species and in relation to cell size. Variability in these factors may be more pronounced in coastal waters (Nelson *et al.*, 1993; Bricaud *et al.*, 1995; Cleveland, 1995; Arbones *et al.*, 1996)

where gradients in species and physiology may occur over smaller spatial and temporal scales. Several investigators have described an increase in chlorophyll-specific absorption, with decreasing chlorophyll concentrations (Bricaud *et al.*, 1995, 1998; Cleveland, 1995). Such relationships reflect a general trend of decreasing cell size with decreasing chlorophyll concentrations, but are also representative of a relative increase in concentrations of accessory pigments in waters with low chlorophyll concentrations (Bricaud *et al.*, 1995, 1997; Sakshaug *et al.*, 1997; Ciotti *et al.*, 1999).

The performance of semi-analytical models in describing relationships of ocean colour to chlorophyll (Carder *et al.*, 1999) and diffuse attenuation (Ciotti *et al.*, 1999) has been shown to be sensitive to variations in the chlorophyll-specific absorption coefficients that accompany changes in phytoplankton cell size and pigment composition. In addition, examination of large data sets from laboratory and field studies has shown that a metric related to phytoplankton cell size can be used as a parameter to explain a large proportion of the variation in the shape of the phytoplankton absorption spectrum (Ciotti *et al.*, 2002). These prior studies did not explicitly separate the relative contributions of pigment packaging and accessory pigment effects, but instead relied on the fact that variations in cell size and accessory pigmentation co-vary in a predictable manner (Ciotti *et al.*, 1999, 2002; Trees *et al.*, 2000).

Knowledge of the extent to which variations in pigmentation related to taxonomic and physiological variations can account for residual variation in size-based empirical relationships may help in refining semi-analytical models and may improve our understanding of the basis for variations in phytoplankton spectral absorption. Variations in accessory pigment concentrations and composition, exclusive of packaging effects, can have a substantial impact on chlorophyll-specific absorption, particularly in the blue region of the spectrum. Prior studies have estimated that 14–42% of the variation in chlorophyll-specific absorption at 440 nm can be attributed to pigment composition effects (Babin *et al.*, 1996; Lazzara *et al.*, 1996; Allali *et al.*, 1997; Stuart *et al.*, 1998).

Information about the absorption properties of individual pigments can be derived by decomposition of phytoplankton absorption into bands attributable to individual pigments. The observed features can then be normalized to pigment concentrations determined by high-performance liquid chromatography (HPLC) to obtain weight-specific absorption coefficients for pigments in their particulate form, $a^*_i(\lambda)$ (m^2 mg pigment^{-1}). Methods that have been applied to the decomposition of *in vivo* phytoplankton absorption spectra into contributions by pigment groups include derivative analysis (Bidigare *et al.*, 1988, 1989), spectral reconstruction methods (Bidigare *et al.*, 1990; Babin *et al.*, 1996; Allali *et al.*, 1997) and the Gaussian decomposition approach (Hoepffner and Sathyendranath, 1993). We chose to use the Gaussian model because it is firmly rooted in the physical processes of electronic absorptions and can be used to reduce hyperspectral data to a series of Gaussian curves with almost no loss of information (Cloutis, 1996). The Gaussian model is relatively insensitive to noise, and Gaussian bands can be adjusted based on the pigments known to be present (Hoepffner and Sathyendranath, 1993).

The objective of this research was to characterize variability in phytoplankton pigment spectral absorption in coastal and offshore waters as it relates to community size structure and pigment composition. Because the method of measurement of phytoplankton absorption can influence the results, two different approaches were used to characterize spectral absorption, the conventional Quantitative Filter Technique (Bricaud and Stramski, 1990; Mitchell, 1990) and the Transmittance–Reflectance method of Tassan and Ferrari (Tassan and Ferrari, 1995). Our study was conducted in shelf waters off North Carolina and western Florida, which provided a range of conditions from mesotrophic coastal waters dominated by larger phytoplankton to picophytoplankton-dominated oligotrophic waters. Using the Gaussian decomposition method, we address the relative importance of package effects and pigment composition in contributing to variations in spectral absorption.

METHOD

Sampling was conducted aboard the 'R/V Edwin Link' as part of the Naval Research Laboratories Spectral Signatures Project in shelf waters off North Carolina and western Florida. Sampling off North Carolina was conducted from May 5, 1997 to May 22, 1997. Stations were located south of the entrance to Chesapeake Bay between 36° and 37°N latitude and within the 50 m isobath (Figure 1). Comparisons between stations in the plume during Leg 1 (May 5–17, 1997) and Leg 2 (May 19–23, 1997) served to highlight temporal differences related to variations in wind forcing. Another set of cruises was conducted off west Florida near Tampa Bay (Figure 2). The first leg was from October 19–22, 1998 and the second leg was from October 26–30, 1998.

Water samples were collected using 16 litre Niskin bottles mounted on a CTD/rosette system. At selected stations, samples were size-fractionated by combining water from two Niskin bottles into a 20 litre carboy. Aliquots from this pooled sample were subsequently subjected to different size-fractionation treatments.

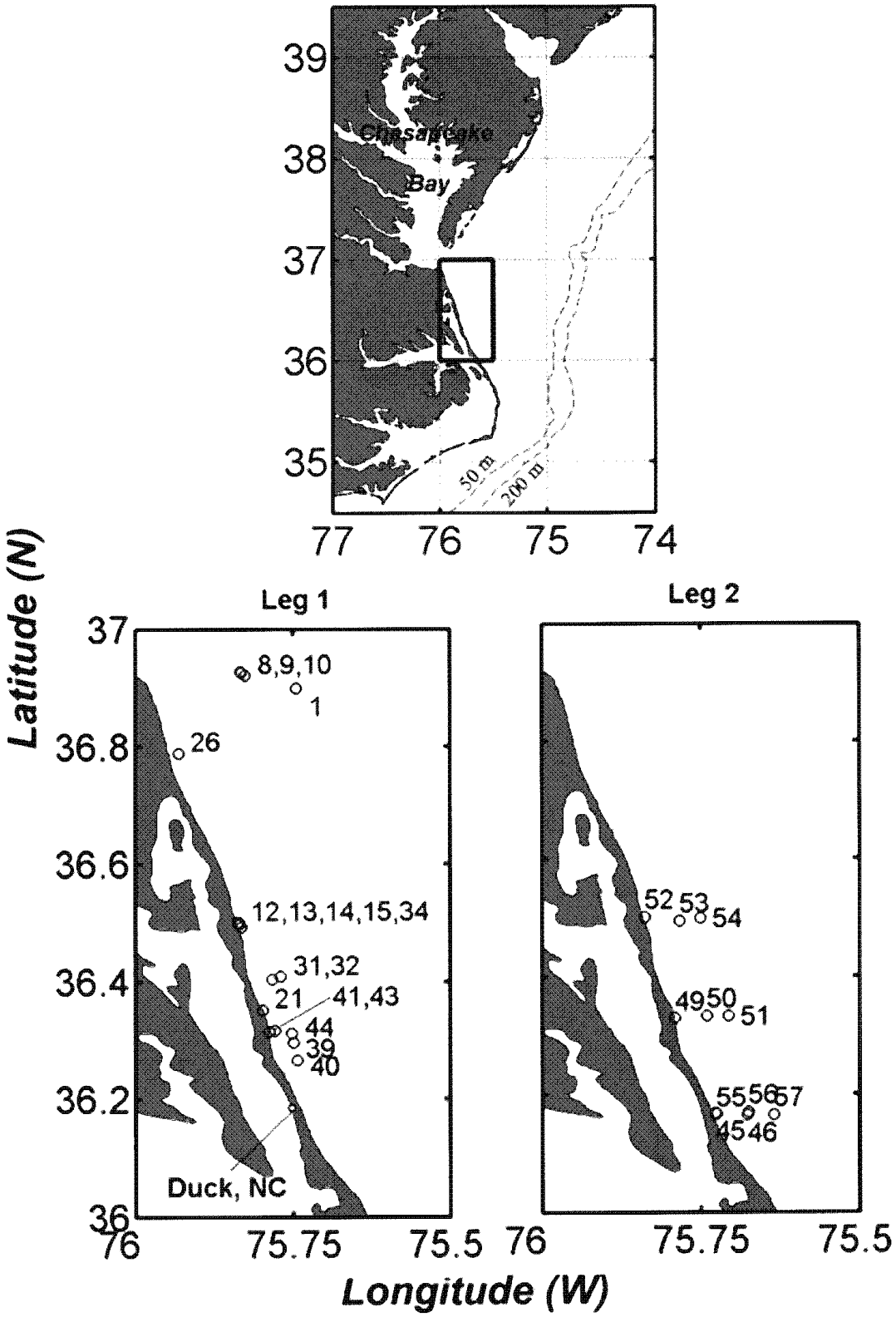

Fig. 1. Sampling during the May 1997 'R/V Edwin Link' cruise occurred in inner shelf waters off the North Carolina coast and south of the mouth of Chesapeake Bay. The enlarged maps show station locations for Leg 1 and Leg 2.

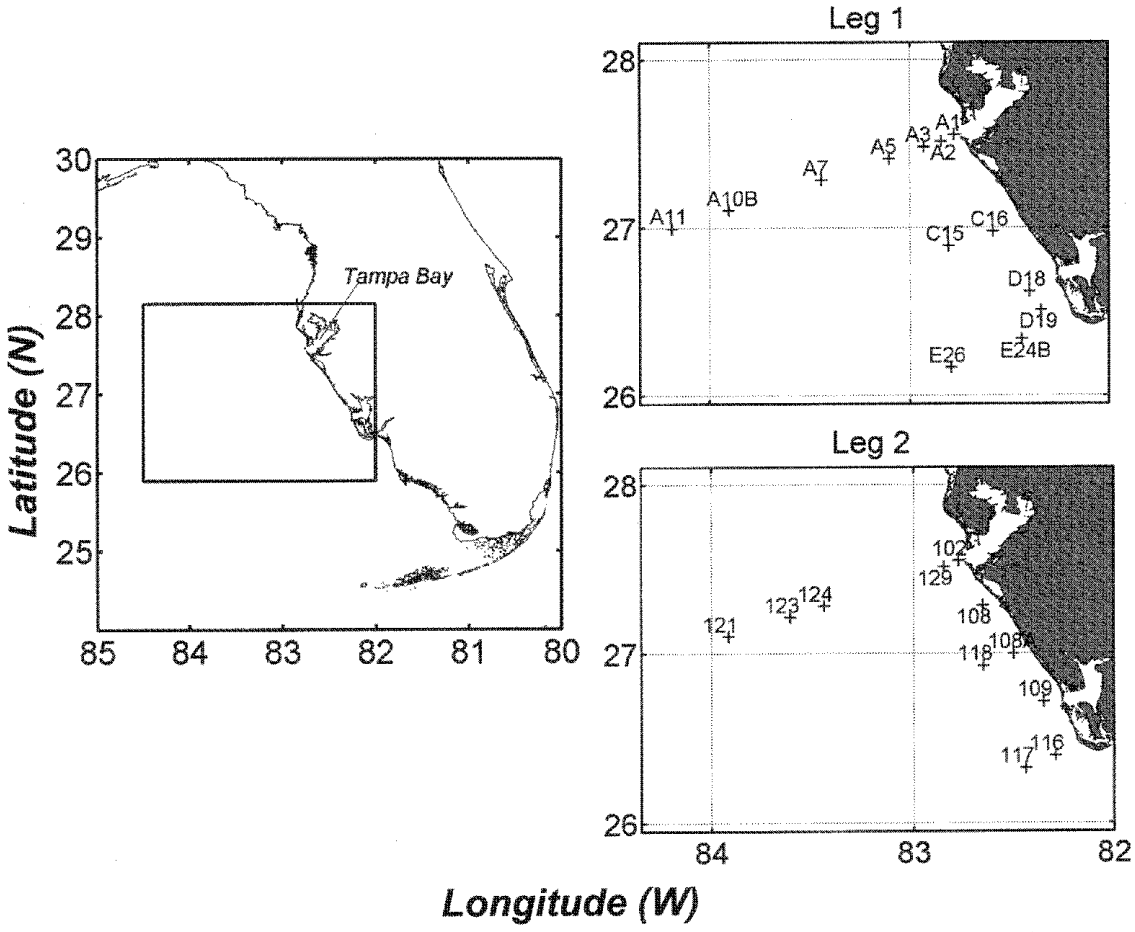

Fig. 2. The October 1998 'R/V Edwin Link' cruise sampled in West Florida shelf waters off Tampa Bay. The enlarged maps show station locations for Leg 1 and Leg 2.

Treatments included an unfractionated sample, a sample passed through 20 μm nylon mesh, and samples filtered through 8 and 3 μm polycarbonate membrane filters (Poretics) housed in 47 mm diameter in-line filtration cartridges.

Pigment analysis

Samples for analysis of photosynthetic pigment concentrations were filtered onto 25 mm diameter Whatman GF/F glass fibre filters. The volumes filtered were generally between 0.2 and 0.6 l. Filters were stored in liquid nitrogen until analysis. For the analysis of phytoplankton chlorophylls and carotenoids, the filters were cut into small strips and the strips were placed in 1 ml of 100% acetone in a 1.2 ml plastic microcentrifuge tube. The samples were then sonicated for 10 s using a Fisher Scientific Model 60 Sonic Dismembrator. A small hole was pierced in the tip of the plastic tube. The samples were centrifuged, expelling the acetone out of the plastic microcentrifuge tube into a glass centrifuge tube. The above procedure was repeated using an additional 1 ml of acetone and then using 1 ml of 100% methanol to give 3 ml of total extract. The total pigment extract was filtered through a 0.2 μm Gelman nylon syringe filter (Acrodisc 13). Extracts were then analysed for pigment content using a tertiary gradient, reverse phase HPLC technique (Wright *et al.*, 1991). Pigments were detected using a Waters 996 Photodiode Array Detector. Two hundred microlitres of the extract was mixed with 100 μl of 0.5 molar ammonium acetate (Ion Pairing Agent) and 200 μl of the extract + Ion Pairing Agent (IPA) mixtures were injected. Violaxanthin and dinoxanthin could not be separated with this technique. The HPLC procedure used in this experiment was found to have a standard error of 8% for chlorophylls and carotenoids. It was subsequently determined that there was incomplete recovery of chlorophylls c_1 and c_2 (hereafter referred to collectively as chlorophyll *c*) from the Gelman nylon Acrodisc filter. A

comparison between filtered and unfiltered samples revealed that recovery of chlorophyll *c* was almost 80%, and no adjustment was made to the data. The separation scheme did not resolve divinyl-chlorophyll *a* from chlorophyll *a*. However, for west Florida shelf samples exhibiting a relatively high chlorophyll *b* : chlorophyll *a* ratio (i.e. >0.2), an additional procedure was performed to quantify the relative amount of divinyl-chlorophyll *a*. The chlorophyll *a* plus divinyl-chlorophyll *a* peak was collected during elution of the sample. At this point, the eluent was ethyl acetate. The sample was diluted 50:50 with Milli-Q and concentrated on a C18 Sep-Pak® (Waters). The pigments were then eluted with 2 ml 100% acetone. The eluent was acidified with 50 µl 0.5 M HCl, and subsequently neutralized with 50 µl of 0.5 M NH_4OH. The solution was then reinjected, and the presence of divinyl chlorophylls was detected as divinyl-phaeophytin-like pigments [cf. (Stuart *et al.*, 1998)]. Unless otherwise specified, the chlorophyll *a* concentration routinely refers to the sum of chlorophyll *a* + divinyl-chlorophyll *a*.

Particulate spectral absorption

Particulate spectral absorption of material concentrated on glass fibre filters was determined by two methods, the conventional quantitative filter pad technique (QFT) as described by Mitchell and by Bricaud and Stramski (Mitchell, 1990; Bricaud and Stramski, 1990), and a combination of transmittance and reflectance measurements (T–R), using an approach modified from that of Tassan and Ferrari (Tassan and Ferrari, 1995). Samples were filtered onto a 25 mm Whatman glass fibre filter and stored in liquid nitrogen until analysis. Measurements were made with a Perkin Elmer Lambda 18 spectrophotometer equipped with a Labsphere 150 mm integrating-sphere (RSA-PE-18 Reflectance Spectroscopy Accessory). For transmittance measurements, filters moistened with filtrate were placed on a quartz slide at the entrance of the sphere and scanned from 350 to 800 nm at a scan speed of 120 nm min^{-1}. Slit width was 2 nm. The mean standard deviation for a series of blanks was approximately 0.0001 m^{-1} for typical filtration volumes. Measurements of reflectance were made with the filters positioned at the back of the integrating sphere. The combination of measurements permitted the application of the method of Tassan and Ferrari (Tassan and Ferrari, 1995) as described in Lohrenz (Lohrenz, 2000). This method accounts for losses as a result of backscatter and eliminates the need for baseline subtraction. Following measurement of transmittance and reflectance of the filters, pigments were extracted from the filter pad using a 15 min extraction in hot methanol. The extracted filters were rinsed with Milli-Q® water to remove residual methanol and phycobiliproteins, and then moistened with seawater filtrate. Measurements of transmittance and reflectance were repeated to obtain the absorption spectrum of the particulate detrital material.

The correction for path-length amplification was done using the following equation (Lohrenz, 2000):

$$a_p(\lambda) = \frac{A(\lambda)}{\beta d_g\left[1 - A(\lambda)\right]} \quad (1)$$

where a_p (m^{-1}) is the corrected absorption coefficient of the particulate material on the filter, and d_g (m) is the geometric path-length, equivalent to the product of volume filtered and the clearance area of the filter. For the QFT method based only on transmittance measurements, $A(\lambda)$ in equation (1) was the absorptance of the filter given by the formula:

$$A(\lambda) = 1 - \frac{T_s(\lambda)}{T_b(\lambda)} \quad (2)$$

where $T'_s(\lambda)$ is the transmittance of the filter with sample and $T_b(\lambda)$ is the transmittance of the blank filter, both adjusted such that the average transmittance at 750 nm was equal to one. A value of β of 2.7 was used to correct for path-length amplification of QFT measurements. For the T–R approach of Tassan and Ferrari (Tassan and Ferrari, 1995), global sample absorption, a_s* (as defined by their equation 13), was substituted for $A(\lambda)$ in equation (1) and a β of 4.8 was used. The values of β were determined from comparisons of filter-pad measurements with measurements of suspensions using an integrating sphere for a variety of phytoplankton cultures and coastal water samples (Lohrenz, 2000).

Spectral absorption as a result of phytoplankton pigments in their particulate form, $a_{ph}(\lambda)$ (m^{-1}), was determined by subtraction of absorption by detrital particulate material (material remaining after methanol extraction), $a_d(\lambda)$, from total particulate spectral absorption, $a_p(\lambda)$. Determination of weight-specific pigment absorption coefficients for major pigment groups was achieved by applying a Gaussian decomposition procedure (Hoepffner and Sathyendranath, 1991) to partition $a_{ph}(\lambda)$ into a set of 13 absorption bands. The algorithm of Sunshine *et al.* (Sunshine *et al.*, 1990) was used to generate the fit. Convergence was considered complete if the root mean square deviation (RMS) between the model and measured spectrum was less than 0.1% of the average absorption, or if the ratio of RMS to average absorption varied within 0.01% for 10 consecutive iterations. The increments in parameters were restricted such that peak width and peak centres were allowed to vary no more than 1 nm between successive iterations. Initial values of the fit parameters along with pigment assignments of

each band are shown in Table I. Initial band heights were estimated by scaling absorption relative to that at 675 nm as shown in Table I. Scale factors were determined from relationships among weight-specific absorption coefficients reported by Hoepffner and Sathyendranath (Hoepffner and Sathyendranath, 1993). A sensitivity analysis revealed that the fit to the data was relatively insensitive to the initial conditions (Carroll, 1999), with the exception of some absorption bands for chlorophylls *b* and *c*. This was attributed to overlap in absorption bands, leading to a 'many-to-one' condition for the solution to the Gaussian fit. Our approach was to use the same set of initial parameters in all cases (Table I), such that relative differences in fitted parameters were related to changes in absorption, rather than differences in initial conditions.

Individual bands were assigned to specific pigment groups based on pigment concentration and wavelength of peak centre. Weight-specific pigment absorption coefficients were determined by fitting the relationship of band peak height to pigment concentration using the following equation (Lutz *et al.*, 1996; Stuart *et al.*, 1998):

$$p_i = \frac{C_i p^*_{mi} p_{mi}}{p_{mi} + C_i p^*_{mi}} \quad (3)$$

where p_i is the peak height of band i, C_i is concentration of the pigment group assigned to that band, p^*_{mi} the weight-specific absorption coefficient corresponding to band i, and p_{mi} is the asymptotic maximum peak height of band i. Curve fits were performed using an interior-reflective Newton curve fitting algorithm (Matlab® v12.1). Unless otherwise specified, all size fractions were included in the curve fit. To evaluate the effects of cell size, curve fits were also performed using data exclusively from the <3 μm size fractions.

Computation of a^*_{sol} and Q^*_a

To examine the influence of pigment packaging on phytoplankton pigment spectral absorption for individual samples, it was necessary to calculate the absorption in the absence of packaging effects, a^*_{sol}. To do this, the band heights for absorption in the absence of pigment packaging, p'_i, were computed as:

$$p'_i = p^*_{mi} C_i \quad (4)$$

where C_i is the pigment concentration corresponding to band i, and p^*_{mi} is the weight-specific absorption coefficient for band i derived from the fit to equation (3). Subsequently, absorption in the absence of packaging effects was determined by summation of the Gaussian functions for each band:

$$a^*_{sol}(\lambda) = \sum p'_i \exp\left[-(\lambda - \lambda_o)^2 / 2\omega^2\right], \quad (5)$$

where λ_o is the centre wavelength (nm) and ω is the peak width parameter (nm). Following the convention of Morel

Table I: Initial input parameters and final mean values for Gaussian fit for North Carolina (NC) and west Florida (WF) shelf waters

	Peak centre (nm)			Peak width (nm)				
Band no.	Initial	Final mean (NC)	Final mean (WF)	Initial	Final mean (NC)	Final mean (WF)	Pigment	Scale factor
1	376	377	376	33	33.8	33.4	Chl *a*	1.7
2	409	410	409	11	13.2	12.4	Chl *a*	0.6
3	435	435	435	15	15.0	14.9	Chl *a*	1.6
4	461	462	461	10	14.8	14.1	Chl *c*	0.3
5	464	465	465	20	21.1	20.6	Chl *b*	0.7
6	490	491	490	21	21.6	21.1	Carot	1.0
7	539	538	540	21	21.1	21.2	Carot	0.5
8	586	589	587	21	20.6	21.0	Chl *c*	0.2
9	622	621	621	13	15.2	14.5	Chl *a*	0.2
10	642	643	642	16	16.0	16.0	Chl *c*	0.2
11	652	651	651	12	12.3	12.0	Chl *b*	0.1
12	675	675	676	11	10.1	10.5	Chl *a*	1.0
13	701	701	701	16	16.3	16.3	Chl *a*	0.1

and Bricaud (Morel and Bricaud, 1981), the effect of packaging on phytoplankton spectral absorption can be represented by the dimensionless ratio:

$$Q_a^* = a_{ph}^*(\lambda) / a_{sol}^*(\lambda), \quad (6)$$

where $a^*_{ph}(\lambda)$ is the chlorophyll *a*-specific absorption cross-section (m^2 mg chlorophyll a^{-1}). Q_a^* has a maximum value of one in the absence of packaging and asymptotically approaches zero with increasing effects of packaging.

RESULTS

Chlorophyll–salinity relationships

Near-surface salinities encountered in inner shelf waters off North Carolina ranged from 24.8 to 33.3 (Figure 3a). Concentrations of chlorophyll *a* were higher for stations in lower salinity surface waters influenced by outflow waters from the Chesapeake Bay. A relatively high concentration of chlorophyll was also observed for the station corresponding to the highest salinity observed, 33.3 (Station 45). Chlorophyll *a* in unfractionated samples showed greater variability than that observed for the <3 mm size fraction (Figure 3a). Near-surface salinities in west Florida shelf waters were generally higher than those off North Carolina, ranging from 31.5 to 36 (Figure 3b). Chlorophyll *a* concentrations were relatively low (<0.2 mg m^{-3}) in high-salinity, offshore waters and increased with increasing salinity. Larger increases were observed for the unfractionated samples as compared with the <3 mm size fraction (Figure 3b). For both North Carolina and Florida shelf waters, the proportion of chlorophyll in the <3 mm size fraction decreased with increasing chlorophyll *a* concentration (Figure 4), an indication that increases in chlorophyll *a* concentrations could be largely attributable to increased relative abundance of larger phytoplankton.

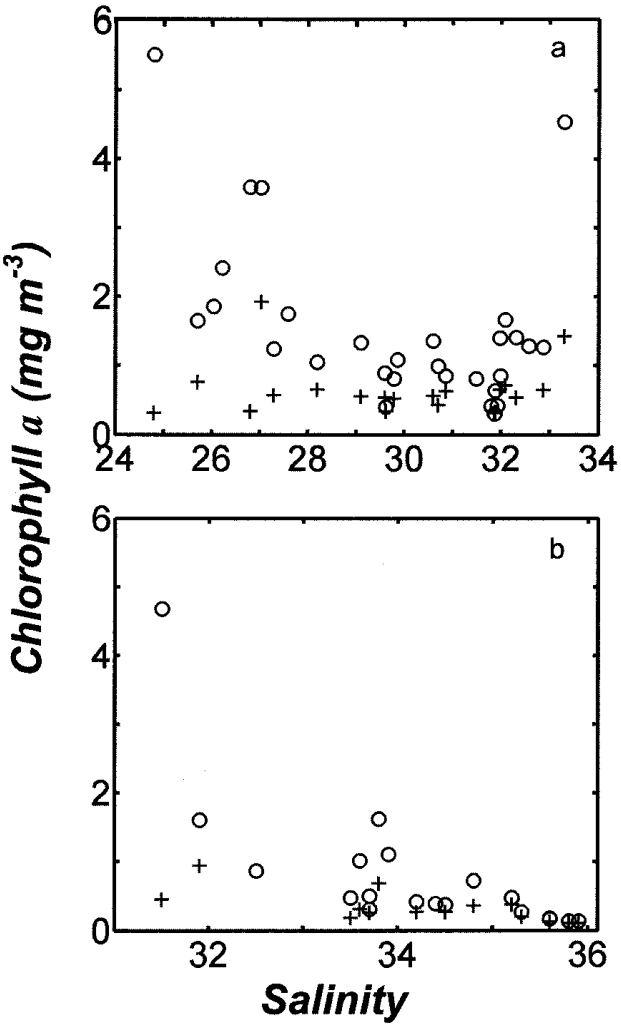

Fig. 3. Chlorophyll *a* increased in the unfractionated samples (○) with decreasing salinity, while there was less of an increase in the <3 μm size fraction (+). (**a**) May 1997, North Carolina shelf; (**b**) October 1998, West Florida shelf.

Pigment spectral absorption

A comparison of the results using the two methods for estimating particulate absorption from filter pad measurements revealed some differences (Figure 5), particularly for the more oligotrophic Station 57. Although spectral shapes were similar, spectra estimated using the T–R method had non-zero absorption at 750 nm, presumably attributable to absorption by detrital material [however, cf. (Babin and Stramski, 2002)]. For Station 52, where the majority of the chlorophyll *a* was associated with cells >3 μm in diameter (Table II), differences between the methods were relatively small (Figure 5a and b). For the higher salinity Station 57, particulate absorption (Figure 5c) and pigment absorption (Figure 5d) were higher for the QFT method. This trend is further illustrated in Figure 6a, where the ratio of $a_{ph}(\lambda)$ measured by the T–R method to that measured using the QFT method is shown for different ranges of chlorophyll concentrations. The largest differences between the methods corresponded to samples with low chlorophyll concentrations, where biomass was dominated by cells <3 μm in diameter (cf. Figure 4). There was no consistent wavelength-dependence in the ratio of T–R to QFT a_{ph} measurements, and mean ratios across the wavelength range of 400–700 nm were well represented by a power function relationship to mean chlorophyll concentration (Figure 6b).

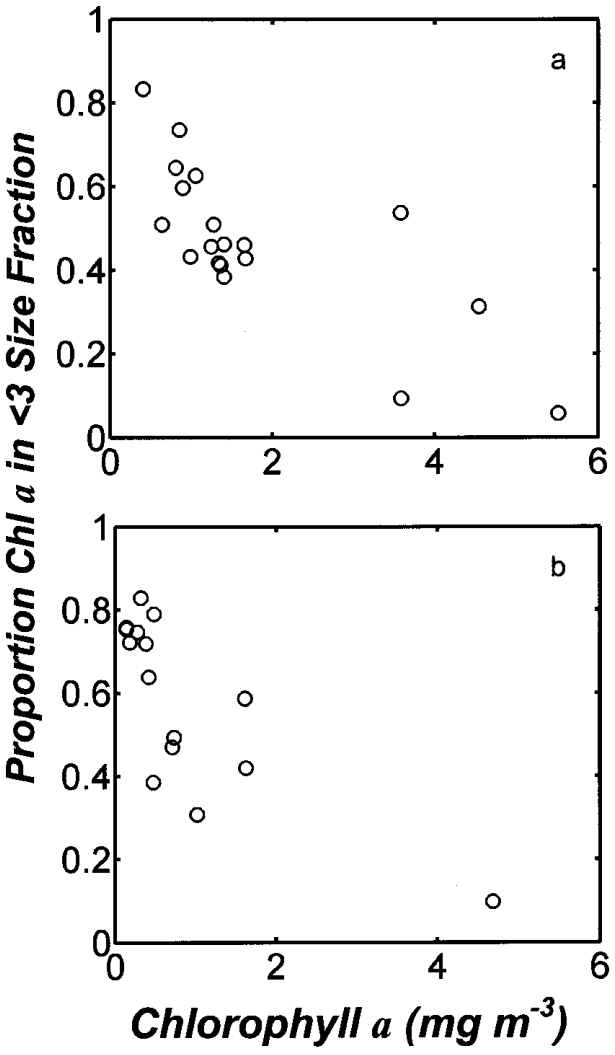

Fig. 4. The proportion of chlorophyll *a* in the <3 μm size fraction generally decreased with increasing chlorophyll *a* concentration. (**a**) May 1997, North Carolina shelf; (**b**) October 1998, West Florida shelf.

The observed differences between the T–R and QFT methods may be attributable to backscattering losses, which would be greater for the QFT method. Theoretical and empirical evidence has demonstrated that the proportion of total particle scattering that is a result of backscattered light (i.e. the particle backscattering ratio) is higher for small particles (Ulloa *et al.*, 1994). Similarly, a comparison of backscattering ratios of different phytoplankton species found relatively high values for small cyanobacteria (Ahn *et al.*, 1992). Studies comparing the T–R method and conventional filter pad technique (Tassan and Ferrari, 1998; Tassan *et al.*, 2000) have shown that values of path-length amplification were less widely dispersed in the case of the T–R method. Therefore, we chose to use the T–R method for all subsequent results. We also provide results derived from the QFT method in selected instances for purposes of comparison. In the case of data collected using the QFT method, the relationship in Figure 6b provides an approximate means by which such data can be compared with that of the T–R method, should that be desired.

A comparison of pigment absorption spectra for stations in North Carolina shelf waters revealed differences among size fractions and water masses (Figure 7). Unfractionated samples at the low-salinity stations impacted by the Chesapeake Bay outflow plume (Figure 7a and c) showed the highest absorption and spectral shapes differed from those of the <3 μm size fractions at these same stations (Figure 7b and d). The spectral shapes of the <3 μm size fractions of Stations 52 and 55 were similar to one another and to those of the unfractionated samples at the higher salinity stations (50 and 57) (Figure 7e and f). All of these spectra exhibited a shoulder in the blue absorption band centred around 460–490 nm and exhibited higher $a_{ph}(440)$:$a_{ph}(676)$ ratios. Based on the Gaussian decomposition of the spectra (Figure 7), the shoulder at 460–490 nm was attributable to higher absorption by carotenoids and chlorophylls *b* and *c* relative to chlorophyll *a*. An examination of ratios of major pigments to chlorophyll *a* revealed that the <3 μm size fractions of Stations 52 and 55 and surface samples from Stations 50 and 57 were characterized by higher ratios of the carotenoids, particularly non-photosynthetic carotenoids (i.e. zeaxanthin, alloxanthin, β-carotene, diadinoxanthin, and diatoxanthin), and accessory chlorophylls (Table II). The ratio of non-photosynthetic carotenoids to chlorophyll *a* was found to be significantly correlated with the $a_{ph}(440)$:$a_{ph}(675)$ ratio for all stations and size fractions ($r^2 = 0.306$; $n = 68$; $P < 0.0001$).

As for the North Carolina shelf, absorption spectra from low salinity, near-shore stations (Stations A1 and 102) on the west Florida shelf showed the highest absorption (Figure 8a and c). Differences between the shapes of these unfractionated spectra and those of the <3 μm size fractions (Figure 8b and d) were subtler than that seen for the North Carolina shelf. Consistent with the observations for the North Carolina shelf, surface samples from the offshore stations (Stations A11 and 121) showed higher ratios of total and non-photosynthetic carotenoids to chlorophyll *a* than that of the inshore stations (Table II). In addition, the ratio of non-photosynthetic carotenoids to chlorophyll *a* was strongly correlated with the $a_{ph}(440)$:$a_{ph}(675)$ ratio for all stations and size fractions ($r^2 = 0.638$; $n = 55$; $P < 0.0001$). Samples from the deep chlorophyll maxima at Stations A11 and 121 were characterized by lower ratios of carotenoids (particularly

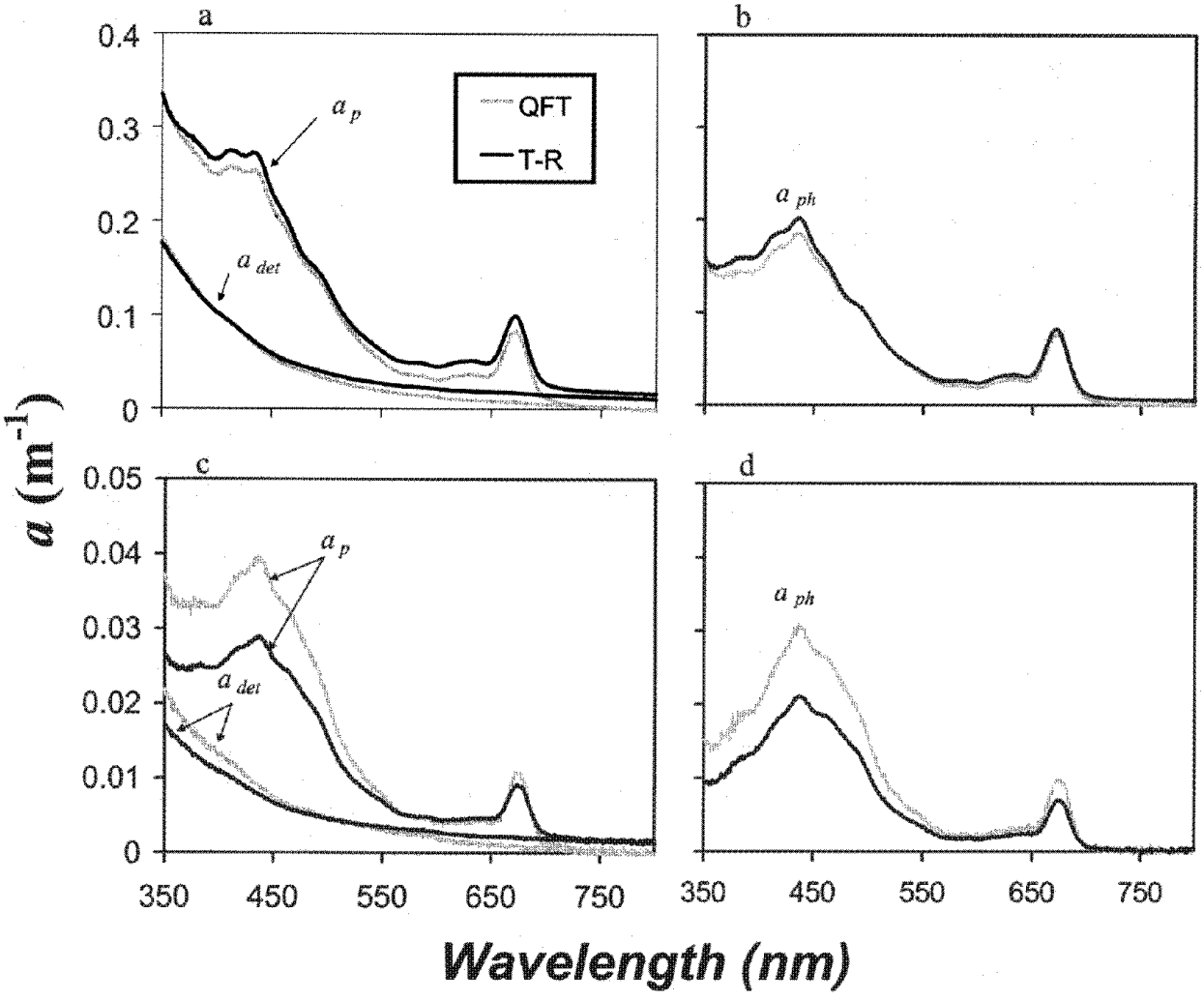

Fig. 5. Comparison of total particulate (a_p), detrital (a_{det}) and phytoplankton pigment absorption (a_{ph}) spectra as estimated by the conventional quantitative filter pad technique (QFT) and by the transmittance–reflectance method (T–R) for the unfractionated near-surface samples from Stations 52 and 57 in North Carolina inner shelf waters. Panels (**a**) and (**c**) show the a_p and a_{det} spectra for Stations 52 and 57, respectively; panels (**b**) and (**d**) display the a_{ph} spectra. Relative differences between methods were smaller for the plume Station 52.

the non-photosynthetic carotenoids) to chlorophyll *a*, but higher ratios of chlorophyll *b* to chlorophyll *a* (Table II). A sample from the deep chlorophyll maximum at Station A11 exhibited a distinct spectral shape (Figure 8f) characteristic of prochlorophytes [cf. (Morel *et al.*, 1993; Moore *et al.*, 1995)]. Quantification of divinyl-phaeophytin-like pigments in acidified extracts revealed that divinyl-chlorophyll *a* accounted for 56% of the chlorophyll *a* + divinyl-chlorophyll *a* of this sample. Prochlorophytes have been shown to have high relative abundance in warm, stratified, low-nutrient waters (Campbell *et al.*, 1998; DuRand *et al.*, 2001; Shalapyonok *et al.*, 2001).

Mean values of the chlorophyll-specific absorption cross-section at 440 nm, $a^*_{ph}(440)$ (m^2 mg chlorophyll a^{-1}), were similar for North Carolina and west Florida shelf regions (Table III). Values for unfractionated samples showed a wide range of variation in both regions. For the T–R method, mean values for the <3 μm size fraction were similar to those for unfractionated samples, but showed a smaller range of variation. Mean values of $a^*_{ph}(440)$ determined using the QFT method were systematically higher than those determined using the T–R method, particularly for the <3 μm size fractions.

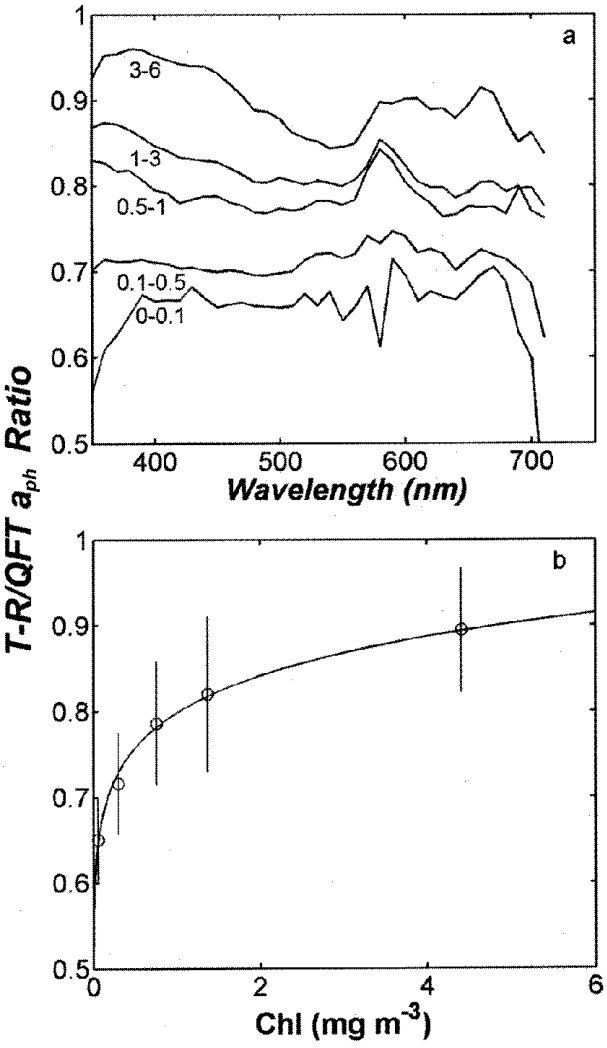

Fig. 6. (**a**) The mean ratio of a_{ph} determined by the transmission–reflectance method (T–R) to that determined by the quantitative filter pad technique (QFT) is shown as a function of wavelength for various chlorophyll concentration ranges (mg m^{-3}). (**b**) Mean values of the T–R:QFT a_{ph} ratio over the wavelength range from 400–700 nm were plotted against the mean chlorophyll concentration for each range shown in (**a**). The data were fitted to a power function (solid curve) described by the equation: $y = 0.798x^{0.0759}$ ($r^2 = 0.993$, $n = 5$).

Pigment composition and phytoplankton taxonomy

Phytoplankton pigment composition and associated taxonomic composition of the phytoplankton community during May 1997 in inner shelf waters off North Carolina showed substantial variation among different water masses (Lohrenz *et al.*, unpublished results). In summary, the carotenoid fucoxanthin was generally the most abundant accessory pigment, particularly for the low salinity stations. Fucoxanthin is a diagnostic pigment found in diatoms, prymnesiophytes, chrysophytes, and some dinoflagellates. Zeaxanthin and chlorophyll *b* were also relatively abundant at most stations. Zeaxanthin is found in cyanobacteria and prochlorophytes; chlorophyll *b* is associated with chlorophytes and prochlorophytes (as divinyl-chlorophyll *b*, although divinyl pigments were not quantified for the North Carolina data). Ratios to chlorophyll *a* of 19′-hexanoyloxyfucoxanthin and peridinin were higher for higher salinity stations. 19′-Hexanoyloxyfucoxanthin is diagnostic for prymnesiophytes, while peridinin is diagnostic of peridinin-containing dinoflagellates.

For the west Florida shelf during October 1998, fucoxanthin was the dominant accessory pigment at the low-salinity stations (A1,102,108,109,129) with a mean ratio to chlorophyll *a* of 0.33 (SE = 0.056, $n = 5$). Zeaxanthin generally dominated in surface waters of all other stations with mean ratios to chlorophyll *a* of 0.46 (SD = 0.060, $n = 19$). For deep offshore populations associated with the subsurface chlorophyll maximum at Stations A7, A10B, A11 and 121, chlorophyll *b* was the dominant accessory pigment (mean ratio to chlorophyll *a* of 0.40, SE = 0.061, $n = 3$) followed by 19′-hexanoylfucoxanthin (mean ratio to chlorophyll *a* of 0.26, SE = 0.048, $n = 3$). Based on results from the acidification procedure, divinyl-chlorophyll *a* accounted for 31–36% of total chlorophyll *a* + divinyl-chlorophyll *a* in surface waters of the offshore stations, and 44–50% in the subsurface chlorophyll maximum.

Gaussian coefficients

Relationships between Gaussian band peak height and pigment concentrations for all stations could be represented by the hyperbolic tangent relationship given in equation (1) (Figure 9). The weight-specific absorption coefficients, p^*_m, and asymptotic maximum peak heights, p_m, for each pigment group and absorption band, along with related statistics, are given in Table IV for the North Carolina stations and Table V for the west Florida shelf. Values of r^2 were generally greater than 0.8 with the exception of some bands, particularly for chlorophylls *b* and *c*. In the case of chlorophyll *c* for North Carolina stations, some outliers were excluded to improve the curve fit (Figure 9). These outliers, and the relatively low r^2 values, were attributed to overlap in absorption bands, particularly chlorophylls *b* and *c*, giving rise to ambiguity as to the assignment of absorption to a specific pigment. Weight-specific absorption coefficients, p^*_m, for the North Carolina and west Florida shelf were generally similar (cf. Tables IV and V). Values of asymptotic maximum peak height, p_m, were systematically higher for the North Carolina shelf stations (cf. Tables IV and V). Values of p_m

Table II: Ratios of major pigment classes for selected stations on the North Carolina (NC) and west Florida (WF) shelves

Water mass	Station	Depth (m)	Size fraction	Salinity	Chl *a* (mg m^{-3})	TC: Chl *a*	NPC: Chl *b*	Chl *b*: Chl *a*	Chl *c*: Chl *a*	a_{ph}(440): a_{ph}(675)
North Carolina										
Plume	52	1.5	Unfrac	24.8	5.5	0.80	0.32	0.02	0.14	2.7
			<3		0.31	1.00	0.59	0.19	0.15	3.2
Plume	55	1.7	Unfrac	26.8	3.6	0.89	0.36	0.02	0.17	2.7
			<3		0.34	0.94	0.48	0.14	0.26	3.0
Shelf	50	3.6	Unfrac	3.6	0.64	1.0	0.56	0.10	0.25	3.1
Shelf	57	2.2	Unfrac	31.86	0.31	1.24	0.66	0.11	0.28	3.1
		18	Unfrac	32.57	1.8	0.90	0.38	0.14	0.17	2.7
West Florida										
Inner Shelf	A1	2	Unfrac	31.90	1.6	0.77	0.51	0.06	n.d.	3.0
			<3		0.95	0.68	0.55	0.06	n.d.	2.7
Inner Shelf	102	2.4	Unfrac	31.50	4.7	0.71	0.21	0.015	0.20	2.4
			<3		0.46	0.63	0.36	0.087	0.15	2.7
Outer Shelf	A11	2.9	Unfrac	35.8	0.14	1.00	0.72	0.06	n.d.	3.2
		67.6	Unfrac	36.6	0.45	0.74	0.30	0.46	n.d.	2.8
Outer Shelf	121	7.2	Unfrac	35.8	0.12	1.04	0.70	0.11	0.20	2.8
		64.3	Unfrac	36.6	0.75	0.86	0.22	0.47	0.37	2.6

Abbreviations used: Chl *a*, chlorophyll *a* + divinyl chlorophyll *a*; TC, total carotenoids; NPC, non-photosynthetic carotenoids; Chl *b*, chlorophyll *b* + divinyl chlorophyll *b*; Chl *c*, chlorophyll c_1+c_2; unfrac, unfractionated.

for the west Florida shelf data were heavily leveraged by a single point (Station 102) at high pigment concentrations.

Parameters derived for data exclusively from the <3 μm size fractions are also given in Tables IV (North Carolina) and V (west Florida). These values were expected to exhibit a reduced level of pigment packaging, and thus approach maximum values. In general, the values of p^*_m were consistent with those derived from the entire data set. Unexpectedly, for the west Florida shelf, values of p^*_m for the <3 μm size fractions were in some cases slightly lower than that observed for the entire data set. In many cases, a reliable value of the asymptotic maximum peak height, p_m, could not be derived because of scatter in the data or insufficient data at high pigment concentrations. In these instances, a linear fit to the data was used.

Gaussian coefficients were derived for absorption data determined using the QFT technique (Table VI) for the purposes of comparison to those derived for absorption measured using the T–R method (Tables IV and V). Values of p^*_m derived for the QFT data were generally higher than those derived from the T–R data. In contrast, the values of p_m were generally similar or lower for data acquired using the QFT method as compared with the T–R method.

Comparison of measured pigment absorption with theoretical values in the absence of pigment packaging

Using the values of p^*_m derived for all size fractions in Tables IV and V, the theoretical levels of absorption in the absence of pigment packaging, $a^*_{sol}(\lambda)$, were calculated for each region using equations (4) and (5). Comparisons were made between the computed $a^*_{sol}(\lambda)$ and measured $a^*_{ph}(\lambda)$ (Figure 10) for unfractionated and <3 μm size fractions for Stations 55 (Cape Hatteras) and 102 (west Florida). Stations 55 and 102 were low-salinity stations with relatively high chlorophyll *a* (Table II). In addition, comparisons were also made for surface and deep chlorophyll maximum samples of the offshore station, Station 121. For the unfractionated low-salinity samples (Figure 10a and c) and for the deep chlorophyll maximum sample (Figure 10f), $a^*_{sol}(\lambda)$ was substantially higher than $a^*_{ph}(\lambda)$, particularly at major absorption

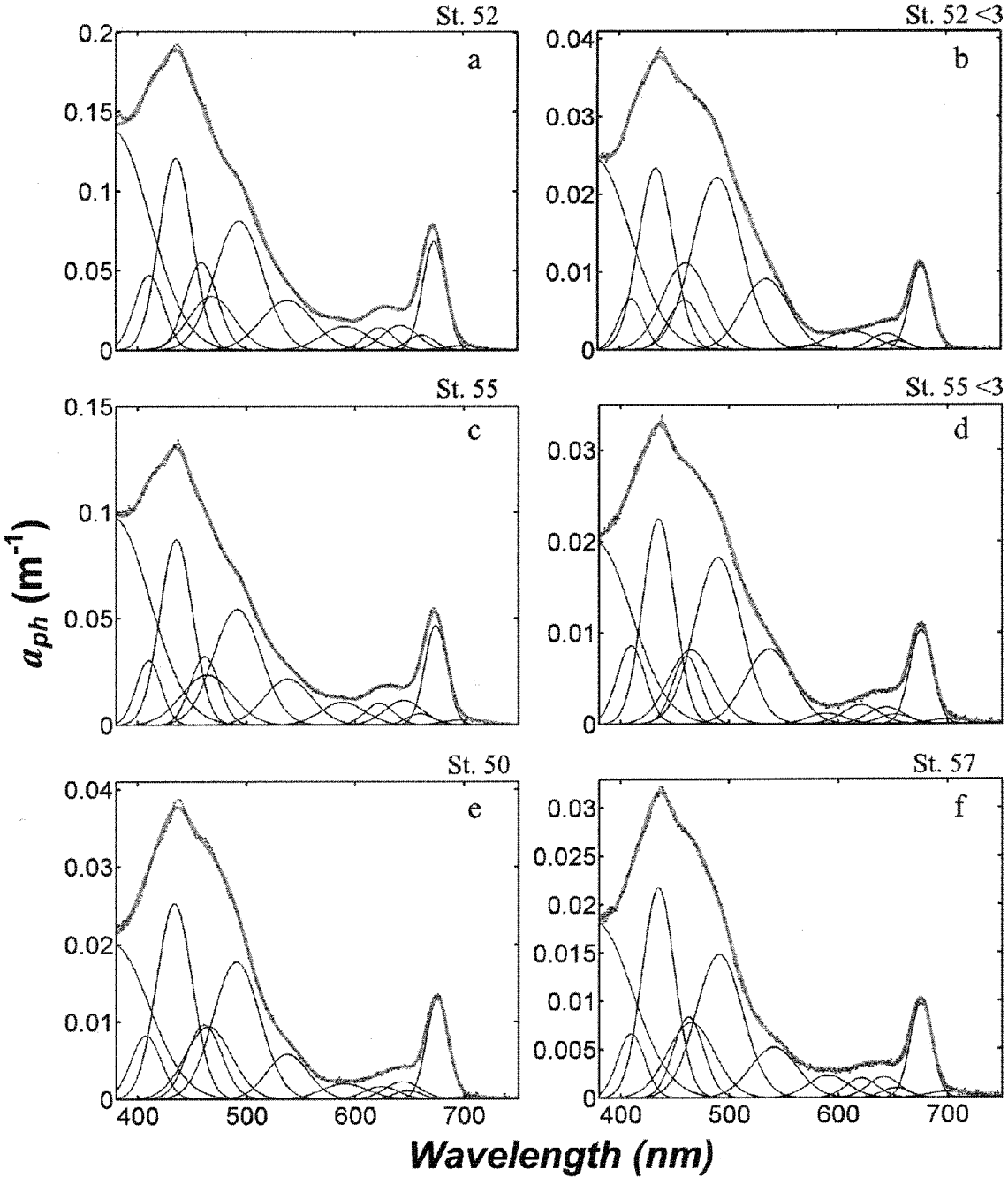

Fig. 7. Phytoplankton pigment absorption spectra from surface samples of selected stations in inner shelf waters off North Carolina during May 1997 are shown, along with fits to a series of Gaussian curves, representative of major pigment absorption bands given in Table I. Spectra of unfractionated water for low-salinity stations 52 (**a**) and 55 (**c**) in the outflow plume of the Chesapeake Bay were higher in overall magnitude and differed in spectral shape compared with the higher salinity stations 50 (**e**) and 57 (**f**). The <3 μm size fractions of stations 52 (**b**) and 55 (**d**) were similar in magnitude and shape to the offshore stations. The thick upper curve in each panel is the modelled fit to the data shown by the dotted line; the overlap in modelled and measured curves was such that they were often indistinguishable. Individual Gaussian bands are shown below each set of spectra. RMS deviation between modelled and measured spectra as a percentage of the average absorption was in all cases less than 0.25%.

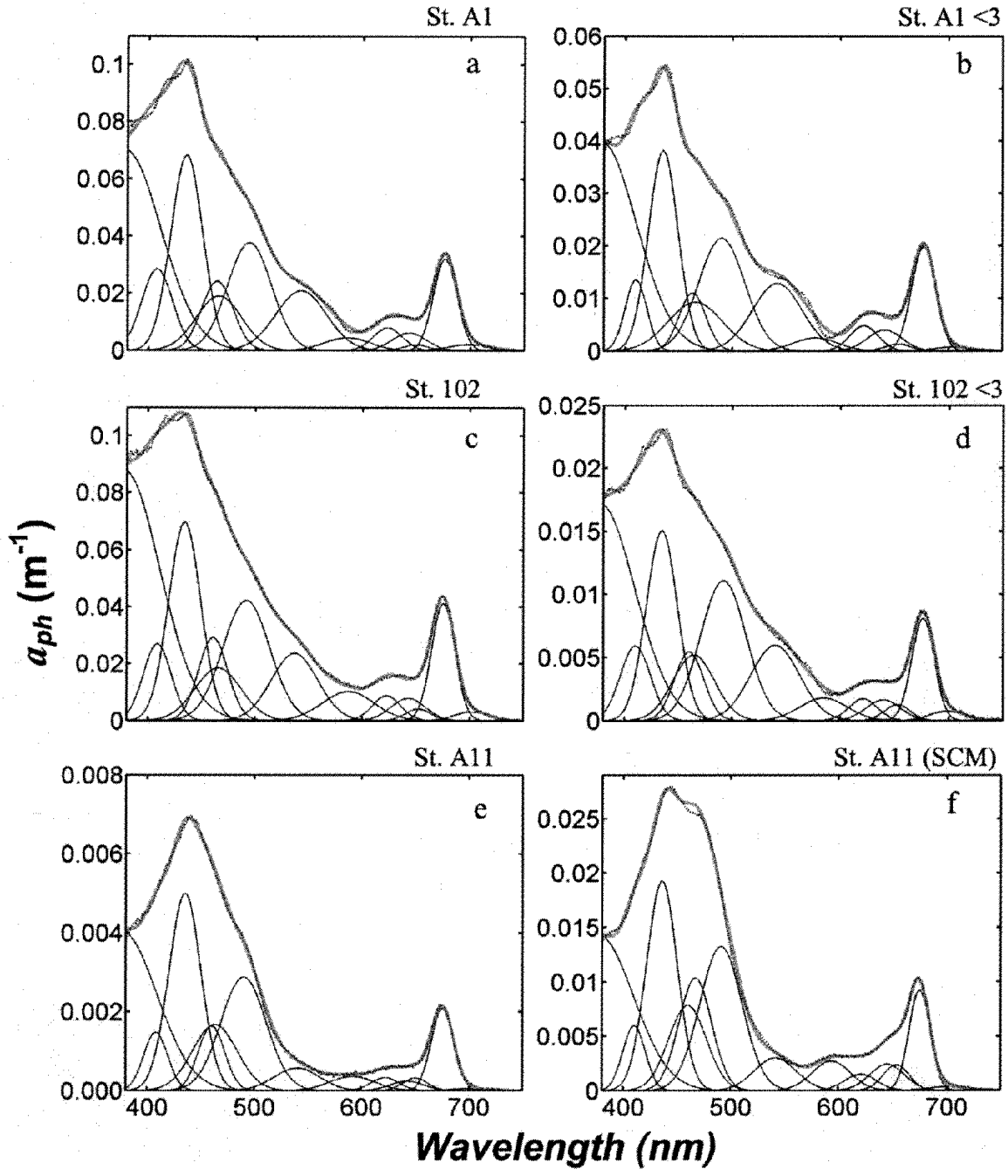

Fig. 8. Phytoplankton pigment absorption from stations sampled in west Florida shelf waters during October 1998 are shown, along with Gaussian curve fits as in Figure 6. Spectra of near-surface samples from Stations A1 and 102, located in low-salinity waters near the mouth of Tampa Bay, were highest in magnitude compared with the <3 μm size fractions of stations A1 (**b**) and 102 (**d**), and to the near-surface samples of the offshore station A11 (**e**). The deep sample from Station A11 (**f**) exhibited an absorption spectrum characteristic of prochlorophytes, the presence of which was confirmed by pigment analyses (see text).

Table III: Chlorophyll a-specific absorption cross-sections at 440 nm, $a^*_{ph}(440)$ in units of m^2 mg chlorophyll a^{-1}, and related statistics for the North Carolina (NC) and west Florida (WF) shelf regions

		T–R method				QFT method				
Region	Size fraction	Mean	SD	Min	Max	Mean	SD	Min	Max	*n*
NC	Unfractionated	0.054	0.014	0.033	0.082	0.066	0.022	0.033	0.104	24
	<3	0.060	0.011	0.045	0.078	0.084	0.017	0.064	0.122	12
WF	Unfractionated	0.050	0.011	0.023	0.074	0.068	0.023	0.018	0.104	28
	<3	0.056	0.008	0.047	0.076	0.082	0.009	0.070	0.101	18

Table IV: Maximum asymptotic band heights (p_m, m^{-1}) and weight-specific absorption coefficients (p^*_m, m^2 mg pigment^{-1}) for major absorption bands fitted to equation (3) for data from the North Carolina shelf region

		All data				<3 only			
Band centre	Pigment	p_m	p^*_m	r^2	*n*	p_m	p^*_m	r^2	*n*
376	Chl *a*	0.37	0.043	0.939	63	0.16	0.046	0.833	13
409	Chl *a*	0.10	0.018	0.861	63	0.095	0.015	0.945	13
435	Chl *a*	0.31	0.045	0.919	63	0.34	0.044	0.958	13
622	Chl *a*	0.047	0.0039	0.979	63	0.019	0.0039	0.852	13
675	Chl *a*	0.18	0.022	0.925	63	0.47	0.020	0.963	13
701	Chl *a*	0.0087	0.0012	0.868	63	0.011	0.00074	0.776	13
464	Chl *b*	–	0.064	0.654	63	–	0.051	0.917	13
652	Chl *b*	–	0.014	0.278	63	0.010	0.018	0.962	13
461	Chl *c*	0.15	0.083	0.858	48*	–	0.072	0.381	9
586	Chl *c*	–	0.019	0.939	48*	–	0.016	0.564	8
642	Chl *c*	0.16	0.020	0.906	46*	–	0.020	0.393	9
490	carot	0.16	0.035	0.866	63	0.20	0.034	0.847	13
539	carot	0.058	0.016	0.844	63	0.031	0.018	0.692	13

*Outliers were excluded (see Figure 9).
Where the value of p_m is indicated as –, a linear regression with intercept forced to zero was used to determine p^*_m. Zero peak height values were excluded. Pigment abbreviations as in Table II.

bands. In contrast, for the <3 μm size fractions of the low-salinity stations (Figure 10b and d) and the unfractionated sample of the offshore station (Figure 10e), differences between $a^*_{sol}(\lambda)$ and $a^*_{ph}(\lambda)$ were smaller. Chlorophyll-specific absorption coefficients of methanol extracts were determined for Station 55. Values of $a^*_{ph}(\lambda)$ were lower than methanol-extractable absorption at major absorption bands for the unfractionated sample (Figure 10a). In contrast, $a^*_{ph}(\lambda)$ was comparable with, or higher than methanol extractable absorption for the <3 μm size fraction (Figure 10b). Values of Q^*_a, calculated from equation (6) for 440 and 675 nm absorption bands, were generally scattered around a value of one for high-salinity surface waters and decreased with decreasing salinity (Figure 11a and c). Values of Q^*_a were also related to the size structure of the phytoplankton population, as

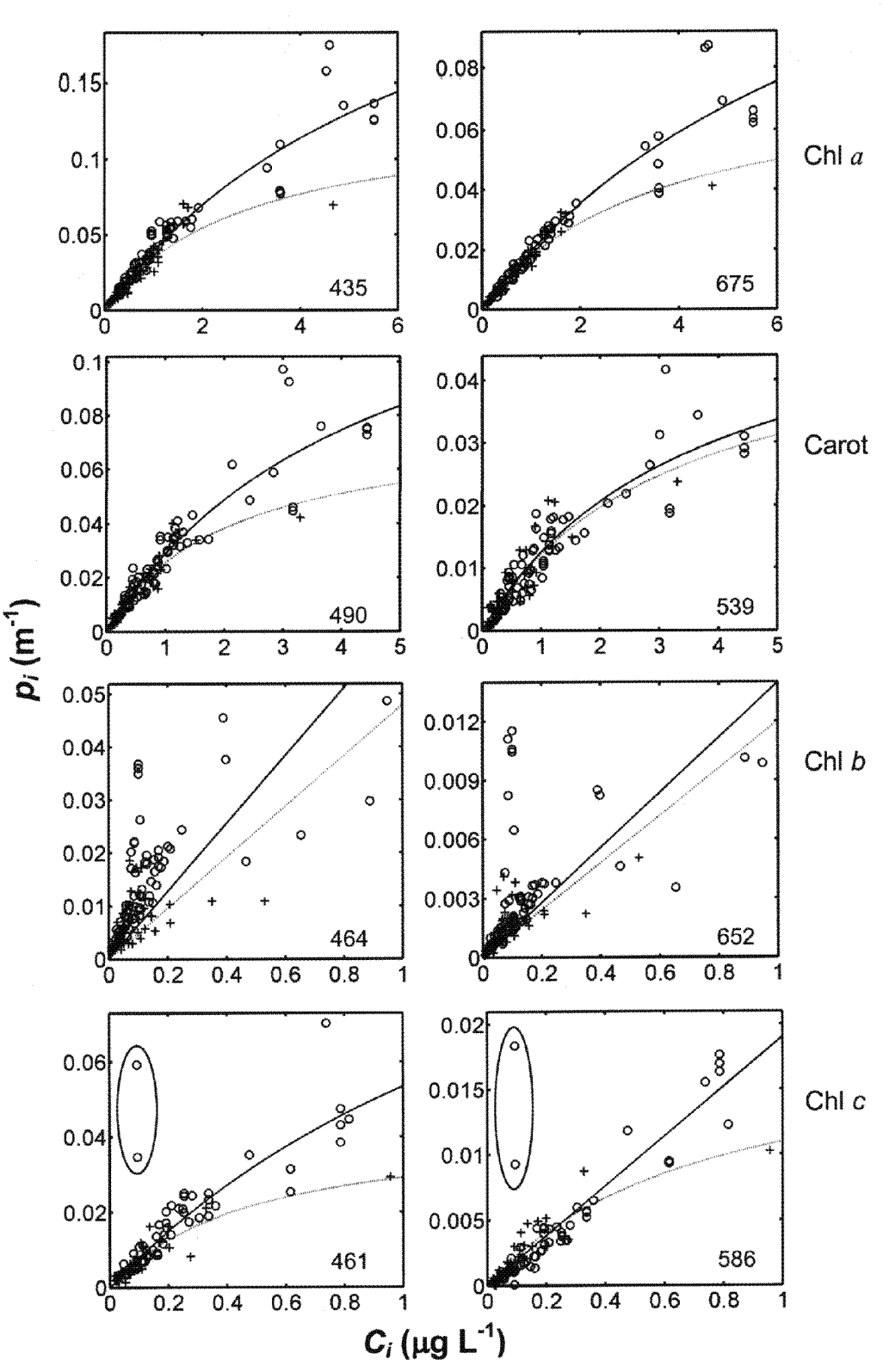

Fig. 9. The relationship of peak heights of Gaussian bands to corresponding pigment concentrations for selected bands is shown for data from North Carolina (○) and west Florida (+) shelf waters during May 1997. Data were fitted either to the hyperbolic tangent relationship given in equation (3) or to a linear regression forced through zero (see Tables IV and V). The curve fit for the Cape Hatteras shelf region was represented by a solid line and for the west Florida shelf by a dotted line.

Table V: Maximum asymptotic band heights (p_m) and weight-specific absorption coefficients (p^*_m) as in Table IV, but for data from the west Florida shelf region

Band centre	Pigment	All data				<3 only			
		p_m	p^*_m	r^2	n	p_m	p^*_m	r^2	n
376	Chl *a*	0.19	0.045	0.898	57	–	0.039	0.940	18
409	Chl *a*	0.054	0.016	0.868	57	–	0.013	0.940	18
435	Chl *a*	0.13	0.047	0.900	57	–	0.039	0.972	18
622	Chl *a*	0.018	0.0048	0.866	57	–	0.0043	0.941	18
675	Chl *a*	0.078	0.023	0.952	57	–	0.020	0.980	18
701	Chl *a*	0.0084	0.0012	0.904	57	–	0.00079	0.733	18
464	Chl *b*	–	0.048	0.220	57	–	0.049	0.311	18
652	Chl *b*	–	0.012	0.508	57	–	0.012	0.779	18
461	Chl *c*	0.043	0.090	0.854	44	0.038	0.087	0.742	13
586	Chl *c*	0.019	0.026	0.871	44	–	0.021	0.772	13
642	Chl *c*	0.011	0.025	0.834	44	–	0.021	0.377	13
490	carot	0.077	0.038	0.906	57	–	0.032	0.956	18
539	carot	0.051	0.016	0.809	57	–	0.016	0.832	18

Table VI: Maximum asymptotic band heights (p_m) and weight-specific absorption coefficients (p^*_m) as in Table IV, but for data acquired by the QFT method for North Carolina and west Florida shelf waters

Band centre	Pigment	North Carolina				West Florida			
		p_m	p^*_m	r^2	n	p_m	p^*_m	r^2	n
376	Chl *a*	0.24	0.062	0.917	62	0.17	0.058	0.903	57
409	Chl *a*	0.096	0.025	0.841	62	0.052	0.021	0.920	57
435	Chl *a*	0.22	0.064	0.848	62	0.11	0.066	0.900	57
622	Chl *a*	0.034	0.0057	0.923	62	0.018	0.0068	0.885	57
675	Chl *a*	0.14	0.030	0.894	62	0.076	0.032	0.946	57
701	Chl *a*	0.0062	0.0019	0.790	62	0.028	0.0012	0.890	57
464	Chl *b*	–	0.075	0.566	62	–	0.066	0.294	57
652	Chl *b*	0.017	0.040	0.494	62	–	0.016	0.594	57
461	Chl *c*	0.15	0.11	0.871	48*	0.025	0.17	0.676	44
586	Chl *c*	0.38	0.019	0.921	48*	0.021	0.030	0.864	44
642	Chl *c*	0.061	0.027	0.934	48*	0.011	0.040	0.773	44
490	carot	0.14	0.051	0.845	62	0.071	0.056	0.903	57
539	carot	0.057	0.022	0.814	62	0.056	0.020	0.786	57

*Outliers were excluded as in Table IV.

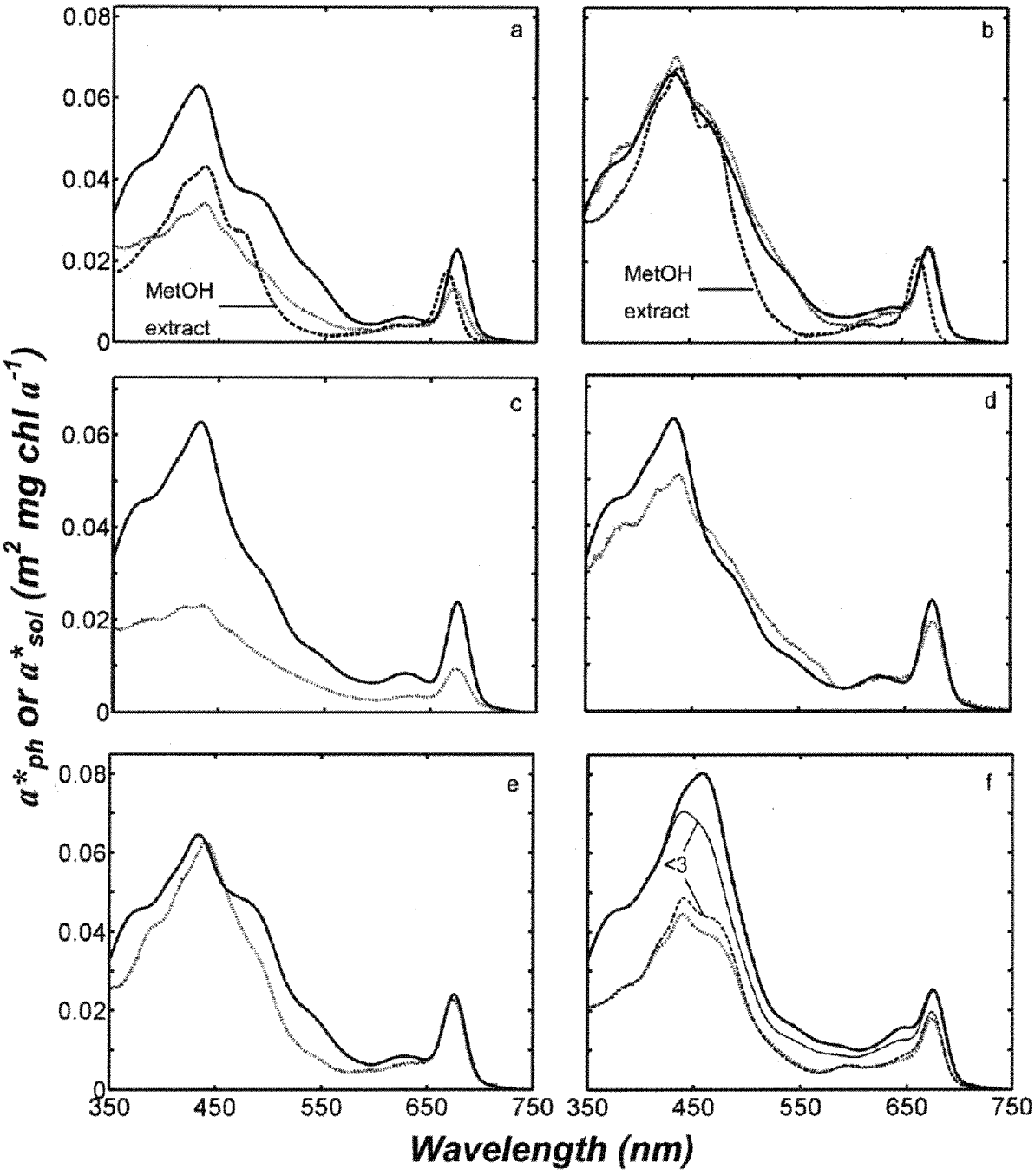

Fig. 10. The relationship between chlorophyll *a*-specific absorption cross-section of intact phytoplankton cells (a^*_{ph}, dotted lines) is shown in comparison with computed values representative of the theoretical absorption in the absence of any packaging effect (a^*_{sol}, thick solid line). Examples included low-salinity stations (**a**) Station 55, North Carolina shelf, 1.7 m, unfractionated, (**b**) Station 55, 1.7 m, <3 μm size fraction, (**c**) Station 102, west Florida shelf, 2.4 m, unfractionated, (**d**) Station 102, 2.4 m, <3 μm size fraction and offshore station, (**e**) Station 121, west Florida shelf, 7.2 m, unfractionated, and (**f**) Station 121, 64.3 m, unfractionated and <3 μm size fractions (<3 μm size fraction represented by thin solid line and thick dashed line). Values of a^*_{sol} were estimated from equations (4) and (5) using weight-specific peak height coefficients given in Tables IV and V. Chlorophyll-specific absorption coefficients of methanol extracts are also shown for Station 55 (**a** and **b**, dashed lines). See Table II for salinities and pigment concentration information.

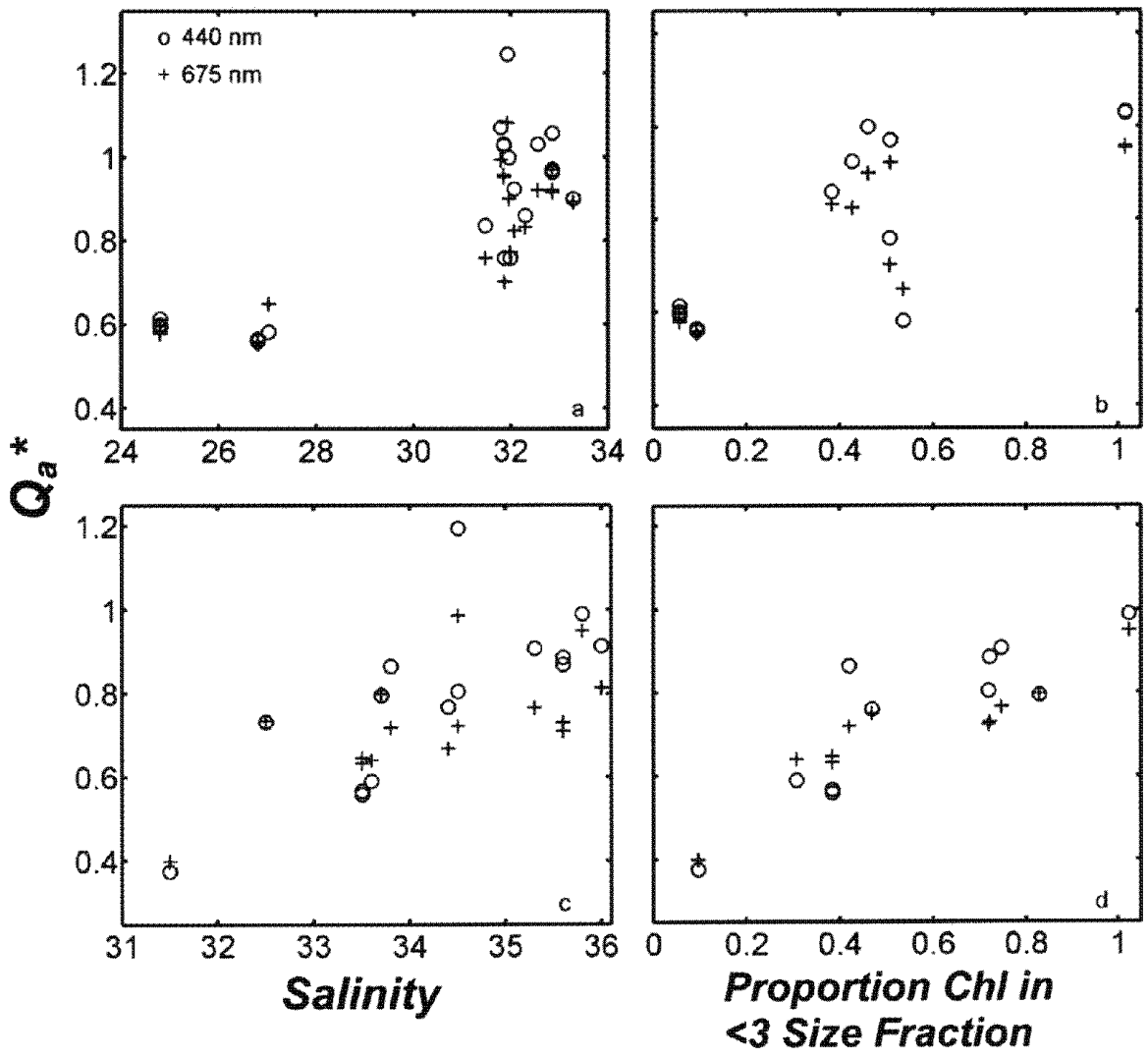

Fig. 11. Ratios of phytoplankton pigment spectral absorption of intact cells to the theoretical absorption in the absence of pigment packaging, Q_a^*, calculated from equation (6), at 440 nm (○) and 675 nm (+) are shown in relationship to salinity (**a**, **c**) and to the proportion of chlorophyll *a* in the <3 μm size fraction (**b**, **d**). Results were for unfractionated samples from North Carolina shelf surface waters during May 1997 (**a**, **b**), and for west Florida shelf surface waters during October 1998 (**c**, **d**).

evidenced by decreasing values of Q_a^* with decreasing proportions of total chlorophyll *a* in the <3 μm size fraction (Figure 11b and d).

Effect of accessory pigment composition on phytoplankton absorption

We next sought to determine the importance of differences in accessory pigment composition as a factor influencing changes in total absorption. To do this, we estimated absorption as a result of pigments other than chlorophyll *a*, $a_{non\text{-}chla}(\lambda)$, by summation of all except the chlorophyll *a* Gaussian absorption bands for each individual spectrum. The ratio of $a_{non\text{-}chla}(440)$ to $a_{ph}(440)$ increased with the increasing ratio of accessory pigments (sum of carotenoids, chlorophylls *b* and *c*) to chlorophyll *a* (Figure 12a) and showed a similar pattern for both North Carolina and west Florida shelf waters. Generally, $a_{non\text{-}chla}(440)$ accounted for between 14 and 28% of total pigment absorption. Values of $a_{non\text{-}chla}(675)/a_{ph}(675)$ for North Carolina shelf waters exhibited considerable scatter in relation to the ratio of chlorophyll *b* to chlorophyll *a* (Figure 12b). In contrast, the absorption ratio for the west Florida shelf data clearly increased with increasing ratio of chlorophyll *b* to chlorophyll *a*. Absorption by pigments

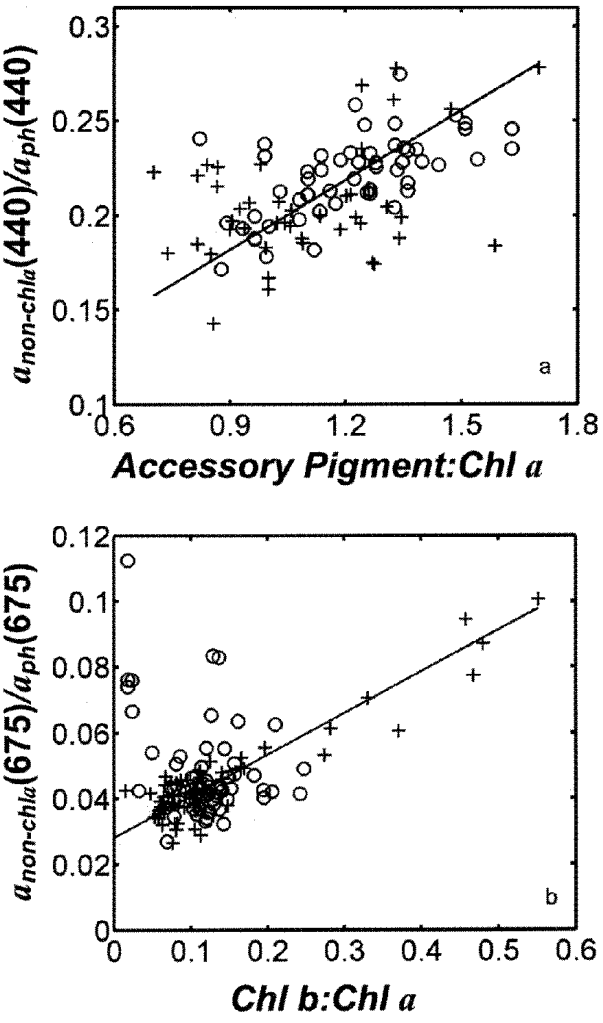

Fig. 12. The ratio of absorption attributable to non-chlorophyll *a* pigments ($a_{non\text{-}chla}$) to total phytoplankton pigment absorption (a_{ph}) at 440 nm increased in relationship to the ratio of total accessory pigments to chlorophyll *a* (**a**) and the ratio at 675 nm increased in relationship to the ratio of chlorophyll *b* to chlorophyll *a*. Symbols: (○), North Carolina shelf, all depths and size fractions; (+), west Florida shelf, all depths and size fractions. The line in (**a**) represents the geometric mean regression (Model II) relationship of all the data and is described by the equation $y = 0.12x + 0.071$ ($r^2 = 0.268$, $n = 99$). The line in (**b**) represents the geometric mean regression relationship of only the west Florida shelf data and is described by the equation $y = 0.13x + 0.028$ ($r^2 = 0.856$, $n = 99$).

other than chlorophyll *a* ranged between 2 and 10% of total absorption at 675 nm.

DISCUSSION

Pigment-specific absorption coefficients

Our study encompassed a wide range of variation in phytoplankton community size structure, taxonomy and pigment composition. Despite the broad range of conditions encountered in the two study regions, relationships between spectral absorption and pigment concentrations were similar, particularly at low pigment concentrations (Figure 9). In general, the relationship of Gaussian band peak heights to pigment concentrations could be described by hyperbolic tangent relationships (Figure 9). The mechanistic basis underlying the hyperbolic tangent relationships can be attributed to an increase in pigment packaging at higher concentrations, because of either an increase in internal pigment concentration within the cell or an increase in cell size (Duysens, 1956; Kirk, 1975; Morel and Bricaud, 1981). Changes in the intracellular organization of pigments within chloroplasts and thylakoid membranes may also be a factor. There was considerable scatter in the relationships between absorption band peak height and pigment concentrations for chlorophylls *b* and chlorophyll *c* (Figure 9). This was particularly problematic for absorption bands in the 460–465 nm region, where chlorophylls *b* and *c*, as well as a variety of non-photosynthetic (photoprotective) carotenoids (Bidigare *et al.*, 1990; Babin *et al.*, 1996), overlap in major absorption features. Stuart *et al.* also reported lower correlation coefficients for relationships between absorption band peak heights and concentrations of chlorophylls *b* and *c* (Stuart *et al.*, 1998).

Based on the observation that values of p^*_m for the <3 μm size fraction data were not systematically higher than values derived for all data (Tables IV and V), we concluded that the p^*_m values derived for all size fractions were representative of maximal values of weight-specific pigment absorption in the absence of pigment packaging. The fact that these values were similar for North Carolina and west Florida shelf waters from different times of the year led us to postulate that these values were representative of inherent absorption properties of major pigment classes in their *in vivo* configuration, rather than being specific to a particular phytoplankton community or photoacclimation response.

In contrast to our observations, Stuart *et al.* observed considerable variation in values of p^*_m between Vancouver coastal waters and the Arabian Sea during different seasonal periods [southwest monsoons and intermonsoon (Stuart *et al.*, 1998)]. Lowest values of p^*_m were associated with eutrophic coastal waters off Vancouver Island and highest values were observed during the intermonsoon in the Arabian Sea, when populations were comprised largely of prochlorophytes and cyanobacteria. Parameters derived for our data were generally within the range of values reported by Stuart *et al.* (Stuart *et al.*, 1998) (Table VII).

The fact that Stuart *et al.* observed a wider range of variation in p^*_m in their study could be attributed to several

causes (Stuart *et al.*, 1998). Firstly, it is possible that their data encompassed a larger range of conditions and different community types than our study. For example, the results of Stuart *et al.* included some samples dominated by prochlorophytes. Prochlorophytes were present in only a small number of our samples, and they were generally not dominant. However, our samples were from distinct regions (North Carolina and west Florida) and included a diverse range of water mass types, phytoplankton community composition and size structure, from diatom-dominated coastal waters to picophytoplankton-rich populations in offshore waters. Based on theoretical arguments, Stuart *et al.* concluded that package effects could have accounted for the differences they observed in weight-specific absorption coefficients among regions (Stuart *et al.*, 1998). If there had been a systematic effect of packaging in our results, we would have expected larger coefficients derived for the <3 μm size fraction data (Tables IV and V). Generally, differences were relatively small, with no indication that coefficients were systematically higher for the <3 μm size fraction data.

To determine the extent to which derived values of maximum asymptotic band height (p_m) and weight-specific absorption coefficient (p^*_m) would vary for populations of different size or taxonomic composition, we subdivided the data based on size fraction and pigment ratio characteristics and determined values of p_m and p^*_m for chlorophyll *a* at 435 nm (Table VIII). Coefficients derived for only unfractionated samples were similar to those for all size fractions given in Tables IV and V, indicating that the inclusion of size-fractionated data in the analyses did not significantly alter the results. Stuart *et al.* used ratios of fucoxanthin:chlorophyll *a* to separate samples comprised of predominately large diatoms from those containing other smaller phytoplankton (Stuart *et al.*, 1998). In an analysis of our data separated according to fucoxanthin:chlorophyll *a* ratios of >0.2 and <0.2, differences were generally less than 20% (Table VIII). This is in contrast to the findings of Stuart *et al.* that samples with fucoxanthin:chlorophyll *a* ratios of <0.2 had substantially higher values of p^*_m (Stuart *et al.*, 1998). We also partitioned data using zeaxanthin:chlorophyll *a* ratios on the basis that samples dominated by cyanobacteria or prochlorophytes would be characterized by high zeaxanthin : chlorophyll *a* ratios. We found lower values of p^*_m for samples with zeaxanthin:chlorophyll *a* ratios of <0.1 (Table VIII). The underlying reason for such low values could be increased packaging. Most of the samples having low zeaxanthin:chlorophyll *a* ratios came from deep subsurface chlorophyll maxima, where photoacclimation would have led to increases in cellular pigmentation and associated increases in packaging effects. Alternatively, taxonomic differences in *in vivo* chlorophyll *a*-specific absorption may exist because of photochemical differences of chlorophyll *a* associated with different pigment–protein complexes (Johnsen *et al.*, 1994). Finally, it must be recognized that the Gaussian decomposition may not entirely isolate absorption because of chlorophyll *a* at 435 nm from other accessory pigments. The Gaussian decomposition method reduces a given absorption spectrum into a series of absorption bands, which are subsequently assigned to individual pigments. An assumption of this approach is that each absorption band can be uniquely associated with a single pigment. It is possible that variability in absorption at 435 nm by other pigments (e.g. zeaxanthin) may have contributed to the differences in p^*_m for chlorophyll *a* at 435 nm. Evidence to support this was the fact that our values for 'unpackaged' weight-specific pigment absorption were generally higher for the blue absorption bands for the chlorophylls than those reported by Bidigare *et al.* [(Bidigare *et al.*, 1990) Table VII]. The Bidigare *et al.* coefficients were determined from laboratory spectra of pigment standards, that were subsequently shifted to match *in vivo* absorption spectra. Our coefficients for the chlorophylls may have been higher as a consequence of the incorrect assignment of absorption by carotenoid pigments to the chlorophyll absorption bands. Alternatively, it is possible that the use of extinction coefficients for solvent extracts of pigments may have led to an underestimation of *in vivo* absorption coefficients for the chlorophylls in the Bidigare *et al.* study.

Another potential source of differences among studies has to do with methods to measure particulate absorption on filters. To examine this, we compared values of p^*_m derived for data from the T–R method with that acquired with the QFT method, the latter being similar to that used by Stuart *et al.* (Stuart *et al.*, 1998), with the exception that Stuart *et al.* adjusted their path-length amplification according to the proportion of divinyl-chlorophyll *a* present in the sample. Our values derived for the QFT data were consistently higher than those derived using the T–R method (cf. Table VI with Tables IV and V), and were still within the range of values reported by Stuart *et al.* (Stuart *et al.*, 1998). We observed a larger difference in chlorophyll *a*-specific absorption cross-section between unfractionated and <3 μm size fraction data for the QFT method than for the T–R method (Table III). Thus, either the T–R method as used here tends to underestimate absorption for samples dominated by smaller cells, or the QFT method is more sensitive to particle size variations, tending toward higher values for samples with increasing relative abundance of small cells. Tassan and colleagues reported that values of path-length amplification were less widely dispersed among different types of samples in the case of the T–R method, which could explain the smaller differences among size fractions for that method

Table VII: Weight-specific absorption coefficients (p^*_m, m^2 mg pigment^{-1}) at selected wavelength bands determined by various studies

Band centre (nm)	Pigment	p^*_m	Source
435	Chl *a*	0.039–0.047	This study
440	Chl *a*	0.026	(Bidigare *et al.*, 1990)
435	Chl *a*	0.034–0.082	(Stuart *et al.*, 1998)
461	Chl *c*	0.083–0.090	This study
462	Chl *c*	0.070	(Bidigare *et al.*, 1990)
461	Chl *c*	0.094–0.30	(Stuart *et al.*, 1998)
464	Chl *b*	0.048–0.064	This study
470	Chl *b*	0.035	(Bidigare *et al.*, 1990)
464	Chl *b*	0.077–0.20	(Stuart *et al.*, 1998)
490	carot	0.034–0.038	This study
490	carot (photosynthetic)	0.037	(Bidigare *et al.*, 1990)
490	carot (non-photosynthetic)	0.053	(Bidigare *et al.*, 1990)
490	carot	0.028–0.081	(Stuart *et al.*, 1998)
675	Chl *a*	0.020–0.023	This study
675	Chl *a*	0.023	(Bricaud *et al.*, 1983)
674	Chl *a*	0.020	(Bidigare *et al.*, 1990)
675	Chl *a*	0.023–0.026	(Johnsen *et al.*, 1994)
675	Chl *a*	0.024–0.037	(Stuart *et al.*, 1998)

Abbreviations as in Table II.

Table VIII: Maximum asymptotic band heights (p_m) and weight-specific absorption coefficients (p^*_m) for chlorophyll a (m^2 mg chlorophyll a^{-1}) at 435 nm for subsamples of data selected based on different size fraction and pigment ratio criteria

	NC				WF			
Treatment	p_m	p^*_m	r^2	n	p_m	p^*_m	r^2	n
Unfractionated only; all stations	0.30	0.042	0.909	24	0.12	0.046	0.878	28
All size fractions; fuco:chl *a* >0.2	0.26	0.043	0.957	33	0.11	0.044	0.906	11
All size fractions; fuco:chl *a* <0.2	1.06	0.041	0.975	30	–	0.038	0.966	46
Unfractionated only; fuco:chl *a* >0.2	0.31	0.036	0.960	16	0.11	0.044	0.899	8
Unfractionated only; fuco:chl *a* <0.2	1.16	0.040	0.991	8	–	0.037	0.937	20
All size fractions; zeax:chl *a* >0.1	0.35	0.046	0.935	46	–	0.037	0.953	52
All size fractions; zeax:chl *a* <0.1	0.48	0.036	0.797	17	0.12	0.037	0.997	5
Unfractionated only; zeax:chl *a* >0.1	0.32	0.045	0.953	14	–	0.036	0.928	24
Unfractionated only; zeax:chl *a* <0.1	0.62	0.031	0.825	10	0.12	0.037	0.997	4

fuco, fucoxanthin; zeax, zeaxanthin.

[(Tassan and Ferrari, 1998; Tassan *et al.*, 2000) Table VI].

Package effects

We estimated the magnitude of package effects by comparing measured spectral absorption with theoretical absorption in the absence of package effects calculated using derived values of weight-specific pigment absorption coefficients. Prior efforts to evaluate packaging in natural populations have relied on spectral reconstruction methods (Nelson *et al.*, 1993; Moore *et al.*, 1995). Such reconstruction methods require adjustments of pigment absorption measured either in solvents or pigment–protein complexes to match that of *in vivo* absorption. An assumption of our approach for estimating the magnitude of pigment packaging is that maximum (i.e. unpackaged) weight-specific pigment absorption coefficients are similar for all types of phytoplankton populations included in the analysis. Clearly, this assumption may be questioned. Johnsen *et al.* found differences among chlorophyll *a*–protein complexes in chlorophyll *a*-specific absorption at 675 nm depending on the composition and species, with values ranging from 0.021 to 0.027 m^2 mg chlorophyll a^{-1} (Johnsen *et al.*, 1994). However, this range of variation was similar to the range of values we derived for weight-specific absorption of chlorophyll *a* at 675 nm (0.020 to 0.023 m^2 mg chlorophyll a^{-1}), and is thus comparable with the uncertainties in our estimated values. In addition, Bricaud *et al.* estimated chlorophyll *a*-specific absorption at 675 nm in the absence of package effects by extrapolating the absorption properties of cultures (assumed to have spherical and homogeneous cells) to a null diameter (Bricaud *et al.*, 1983). They determined a maximal value of chlorophyll *a*-specific absorption at 675 nm of 0.023 m^2 mg chlorophyll a^{-1}, comparable with our findings.

Given the assumption that the maximum weight-specific pigment absorption coefficients derived with the Gaussian decomposition procedure were representative of phytoplankton in the populations we examined, we could then assess the magnitude of pigment packaging without intermingling effects of changes in pigment composition. Even when only surface samples were considered (Figure 11) thereby minimizing the potential impact of photoacclimation effects, our findings provide evidence for substantial package effects on absorption (up to 62% decrease) at major absorption bands, particularly at low salinities and for populations dominated by larger phytoplankton (Figures 10 and 11). These findings are consistent with the conclusions of other authors regarding the importance of package effects in natural populations (Bricaud *et al.*, 1995; Cleveland, 1995; Allali *et al.*, 1997; Stuart *et al.*, 1998).

We also observed a considerable reduction in absorption (~40% at 440 nm and ~30% at 675 nm) in the case of the west Florida sample from the deep chlorophyll maximum at Station 121 (Figure 10f). Package effects were evident in this sample even for the <3 μm size fraction, although smaller in magnitude (~32% at 440 nm and 22% at 675 nm). A high ratio of chlorophyll *b*:chlorophyll *a* (0.47) was indicative of a substantial prochlorophyte population in the sample, with about 60% of the total chlorophyll *a* + divinyl chlorophyll *a* present in the <3 μm size fraction. These results support claims by other investigators that under low-irradiance conditions package effects may be substantial even for populations dominated by small cells (Lazzara *et al.*, 1996; Bricaud *et al.*, 1999). As stated previously, it is possible that weight-specific pigment absorption coefficients derived for data from all samples led to an overestimation of packaging for this deep population. To examine this question, coefficients derived for data exclusively from samples with low zeaxanthin:chlorophyll *a* ratios (<0.1) were used to estimate unpackaged absorption for this sample and compared with the measured absorption spectrum (data not shown). This resulted in a lower estimate of packaging for both the unfractionated sample (19% at 440 nm and 675 nm) and <3 μm size fraction (6% at 440 nm and 11% at 675 nm). Consequently, we must acknowledge that variability in the Gaussian coefficients is a source of uncertainty in our estimation of package effects, and ranges on the order of 20–25%.

Comparisons with methanol extracts provided independent confirmation that package effects were significant for the surface sample at Station 55 (Figure 10a and b). Values of $a^*_{ph}(\lambda)$ were consistently lower than methanol-extractable chlorophyll *a*-specific absorption for the unfractionated sample at Station 52 (Figure 10a), but were higher than, or comparable with the methanol-extractable chlorophyll *a*-specific absorption for the <3 μm size fraction (Figure 10b). The exact relationship of methanol extractable absorption to *in vivo* absorption is difficult to predict, as discussed by Bissett *et al.* (Bissett *et al.*, 1997). Solution effects will not only release pigments from their discrete state within thylakoid membranes, but will also disrupt pigment–protein complexes. This will, in turn, alter the chlorophyll-specific absorption properties of pigments. Extinction coefficients for chlorophyll *a* in methanol are 0.055 at 418 nm and 0.017 m^2 mg chlorophyll a^{-1} at 675 nm (Strain *et al.*, 1963). The methanol-extractable chlorophyll *a*-specific absorption shown in Figure 10a was lower (0.039 m^2 mg chlorophyll a^{-1}) than the extinction coefficient for pure chlorophyll *a* at 418 nm, and was comparable at 665 nm (0.018 m^2 mg chlorophyll a^{-1}). For the <3 μm size fraction of Station 55 (Figure 10b), methanol-extractable chlorophyll *a*-specific

absorption at 418 nm (0.058 m^2 mg chlorophyll a^{-1}) was similar to the extinction coefficient for pure chlorophyll *a*, while methanol-extractable chlorophyll *a*-specific absorption at 675 nm (0.021 m^2 mg chlorophyll a^{-1}) was higher than the extinction coefficient for pure chlorophyll *a*. Higher extractable absorption can be explained by the presence of other pigments, particularly chlorophyll *b*. The chlorophyll *b*:chlorophyll *a* ratio of the <3 μm size fraction was 0.14, compared with 0.02 for the unfractionated sample (Table II). Lower extractable absorption is less easily explained, but may be a result of incomplete extraction, interference with absorption by solvent and other substances or degradation during the extraction process. Despite the difficulties in interpretation of the relationship of methanol extractable-absorption to *in vivo* absorption, the results do provide additional evidence for package effects at Station 55.

The fractional reduction in absorption estimated by our approach exhibited a relationship to size structure of the phytoplankton community (Figure 11b and d). Based on theoretical arguments and simplifying assumptions such as homogeneous pigment distributions within cells and regular geometric cell shapes (Morel and Bricaud, 1981; Sathyendranath *et al.*, 1987), Q_a^* can be approximated using the following relationship:

$$Q_a^* = \frac{3Q_a}{2da_{cm}} \quad (7)$$

where Q_a is the dimensionless efficiency factor for light absorption, d is the cell diameter, and a_{cm} is the absorption coefficient of cellular material. Making the assumption that absorption at 675 nm is due mainly to chlorophyll *a*, $a_{cm}(675)$ can be estimated by the product of intracellular chlorophyll *a* concentration, c_i (mg m^{-3}) and the *in vivo* chlorophyll-specific absorption coefficient at 675 nm, $a^*_{chl}(675)$, here taken as 0.021 m^2 mg chlorophyll a^{-1} based on the average of values in Tables IV and V. Values of Q_a, d, and c_i for algal cultures from a survey of the literature were used to estimate Q_a^* from equation (7) and the results were plotted in relationship to the product of d and c_i (Figure 13). The range of calculated values of Q_a^* was similar to that observed in Figure 11, supporting the validity of our findings. Values in Figure 13 in numerous cases exceeded the theoretical maximum value of one. This could be attributable to various factors. Values of a_{cm} based on chlorophyll *a* would be underestimated if there were significant contributions to absorption by chlorophyll *b* (or divinyl-chlorophyll *b*). Assumptions of homogeneity and sphericity were probably not valid in all cases. Measurement errors may have also contributed. Finally, the value of 0.021 m^2 mg chlorophyll a^{-1} may have been an underestimate of the true *in vivo* absorption properties at 675 nm for some species as discussed previously.

Effects of accessory pigment composition

There is compelling evidence for the importance of package effects in influencing phytoplankton absorption, but what is the role of pigment composition as a factor? Correlations between ratios of non-photosynthetic pigments to chlorophyll *a* and $a_{ph}(440)$:$a_{ph}(675)$ ratios were significant, supporting the view that pigment composition influenced spectral shape. However, such correlations describe intermingled effects of both pigment composition and package effects. To attempt to characterize effects of pigment composition exclusively, we used Gaussian parameters derived for individual spectra to calculate the absorption by non-chlorophyll *a* pigments ($a_{non\text{-}chla}$). The ratio of this calculated absorption to measured total pigment absorption (a_{ph}) at 440 nm did increase with increasing ratios of accessory pigments to chlorophyll *a* (Figure 12a). Non-chlorophyll *a* pigments accounted for between 14–28% of the pigment absorption at 440 nm, with higher values associated with higher ratios of accessory pigments to chlorophyll *a*. Stuart *et al.* estimated a similar percentage (14–31%) by subtracting the Gaussian chlorophyll *a* absorption from the measured total absorption at 440 nm and determining the fraction of absorption remaining (Stuart *et al.*, 1998). It must be acknowledged that the Gaussian method provides only an approximation of spectral absorption characteristics of individual pigments, particularly away from their principal absorption maxima. This may partially account for the scatter in the data in Figure 12a. Stuart *et al.* argued, based on multiple regression analyses, that pigment composition accounted for 29–42% of the variation in chlorophyll *a*-specific absorption at 440 nm, with the balance attributable to pigment packaging (Stuart *et al.*,

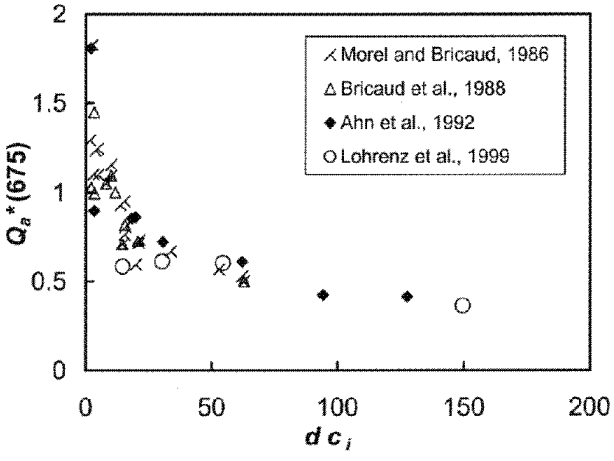

Fig. 13. Values of Q_a^* at 675 nm estimated from published studies of phytoplankton cultures are shown in relationship to the product of cell diameter, d, and intracellular chlorophyll *a* concentration, c_i. Values of Q_a^* were estimated from equation (7) as discussed in the text.

1998). However, the multiple linear regression approach provides an assessment of the amount of variation explained by variations in accessory pigments, but does not address directly their contribution to total absorption.

Numerous other investigators have argued for a significant impact of non-photosynthetic pigments on chlorophyll *a*-specific spectral absorption in the blue region of the spectrum (Babin *et al.*, 1996; Lazzara *et al.*, 1996; Allali *et al.*, 1997; Bouman *et al.*, 2000a). Using a spectral reconstruction approach described by Babin *et al.* (Babin *et al.*, 1996) of partitioning absorption according to concentrations and weight-specific absorption coefficients of photosynthetic and non-photosynthetic pigments, Lazzara *et al.* (Lazzara *et al.*, 1996) determined that variations in non-photosynthetic pigments in tropical North Atlantic waters accounted for about a 20% decrease in chlorophyll *a*-specific absorption. Allali *et al.* (Allali *et al.*, 1997), using a similar approach, reported a larger effect in the subequatorial Pacific of an approximate 30% decrease, while an approximate vertical range in absorption by non-photosynthetic pigments of 20% was reported for equatorial Pacific waters. These changes were larger than the approximately 15% variation in absorption that we observed as a result of non-chlorophyll *a* pigments (Figure 12a). The fact that we observed smaller changes may reflect differences in community species composition and photoacclimation. There are also likely to be inherent differences in the methods used to partition absorption into contributions by pigment groups. For example, the Gaussian approach did not separate contributions by photosynthetic and non-photosynthetic pigments. Offsetting changes in non-photosynthetic pigments and chlorophylls *b* and *c* may have resulted in a smaller overall change. In addition, as stated previously, overlap in absorption bands could have resulted in errors in apportioning absorption to appropriate pigments. Another consideration is that the spectral reconstruction method (Mann and Myers, 1968; Bidigare *et al.*, 1990) relies on assumptions that spectral fine structure and relative extinction characteristics of pigments in solvents are retained in their *in vivo* state, which may not necessarily be the case.

The problem of the contribution to absorption by accessory pigments is less complicated for the absorption band at 675 nm. Here, the primary pigments, other than chlorophyll *a*, are chlorophyll *b* and to a lesser extent, chlorophyll *c*. Results revealed that $a_{non\text{-}chla}$ accounted for generally <10% of total pigment absorption at 675 nm (Figure 12b). The fraction of non-chlorophyll *a* absorption increased with increasing ratio of chlorophyll *b*:chlorophyll *a* in the west Florida shelf data, with the chlorophyll *b*:chlorophyll *a* pigment ratio accounting for 86% of the variation in the ratio of $a_{non\text{-}chla}$ to a_{ph}. There was no significant relationship for the North Carolina shelf data. This was probably because a smaller range in the chlorophyll *b*:chlorophyll *a* ratio was encountered on the North Carolina shelf as compared with the west Florida shelf.

Implications for bio-optical algorithms

Our findings that pigment packaging was responsible for a large proportion of the variation in chlorophyll-specific phytoplankton absorption (Figures 10 and 11) serve as an endorsement of semi-analytical modelling approaches that incorporate information about size structure of phytoplankton communities [e.g. (Carder *et al.*, 1999; Ciotti *et al.*, 1999, 2002)]. An advantage of such semi-analytical approaches over strict empirically based methods is their capability for examining the effects of variation in specific terms, such as phytoplankton community-dependent variations in chlorophyll-specific absorption, on modelled optical properties. Based on our findings, both chlorophyll *a* concentration and salinity provide potentially useful metrics of variations in pigment packaging that accompany changes in phytoplankton size structure in shelf waters (cf. Figures 4 and 11). Our results also provide evidence that information about accessory pigment concentrations and composition may help to further constrain variation in chlorophyll-specific absorption coefficients (cf. Figure 12). Additionally, such information may be useful in interpreting changes in phytoplankton community composition.

The Gaussian method, as used in this study, provides an approach for the determination of pigment concentrations from absorption spectra, measured either using *in situ* instrumentation or remote sensing. Alternatively, in cases where pigment concentrations are known, it may be possible to derive estimates of phytoplankton pigment absorption in support of bio-optical algorithms. The consistency of p^*_m values (Tables IV and V) is encouraging for the potential success of such applications. From the values of r^2 in Tables IV and V, it can be seen that the best capabilities for prediction of pigments from absorption will be for chlorophyll *a*, chlorophyll *c*, and carotenoids. Similarly, in cases where these are the dominant pigments, it should be possible to estimate absorption from pigment concentrations with reasonable accuracy. Uncertainties in estimates of either pigment concentrations or absorption will increase at high pigment concentrations. This assertion is based on the fact that estimates of the maximum asymptotic peak height values, p_m, varied between regions and within a given region for the combined versus <3 μm size fraction data (Tables IV and V). There were also substantial differences in p_m among subsets of data partitioned based on pigment ratios (Table VII). Furthermore, our estimated p_m values were systematically lower than those of Stuart *et al.*

for all data sets examined (Stuart *et al.*, 1998). The wide dispersion in p_m values highlights the need for analyses of additional data sets from coastal waters encompassing wider ranges of pigment concentrations. It may be that p_m values will have to be routinely determined for each region and time to provide reliable estimates of either reconstructed 'packaged' absorption spectra from a given set of pigment data, or alternatively, to estimate pigment concentrations from *in vivo* absorption spectra in areas of high pigment concentrations.

Conclusions

Our results confirm the findings of various other investigators that variations in phytoplankton absorption and its relationship to chlorophyll *a* and other pigments can be substantial. It is widely recognized that variations in non-chlorophyll *a* pigments contribute in some way to such variations, in addition to pigment packaging. Our approach has illustrated the utility of the Gaussian decomposition procedure for quantitative assessments of pigment packaging in natural populations. The results provide evidence that package effects dominated variability (up to 62%) in chlorophyll-specific absorption at 440 and 675 nm. Variations in non-chlorophyll *a* pigments also contributed, but to a lesser extent (14–28%). The Gaussian decomposition method has potential bio-optical applications for estimating pigment concentrations or reconstructing absorption in natural waters. The utility of this approach will become clearer as additional information is gathered about coefficients derived from other regions and times.

ACKNOWLEDGEMENTS

We are grateful for the assistance of the captain and crew of the 'R/V Edwin Link'. Funding for this research was provided by NASA (NAG5-4570, NAG5-9770), by the National Science Foundation through the US JGOFS Synthesis and Modeling Program (OCE-98–18804), and by the Naval Research Laboratory as part of the Spectral Signatures of Optical Properties in the Littoral Zone Program. We thank V. Lochhead and C. Carroll for technical assistance. We are grateful to P. Bissett, S. Sathyendranath, H. Sosik and an anonymous reviewer for helpful comments on earlier versions of this paper.

REFERENCES

Ahn, Y., Bricaud, A. and Morel, A. (1992) Light backscattering efficiency and related properties of some phytoplankters. *Deep-Sea Res. I*, **39**, 1835–1855.

Allali, K., Bricaud, A. and Claustre, H. (1997) Spatial variations in the chlorophyll-specific absorption coefficients of phytoplankton and photosynthetically active pigments in the equatorial Pacific. *J. Geophys. Res.*, **102** (C6), 12413–12423.

Arbones, B., Figueiras, F. G. and Zapata, M. (1996) Determination of phytoplankton absorption coefficient in natural seawater samples: evidence of a unique equation to correct the pathlength amplification on glass-fiber filters. *Mar. Ecol. Prog. Ser.*, **137**, 293–304.

Babin, M. and Stramski, D. (2002) Light absorption by aquatic particles in the near-infrared region. *Limnol. Oceanogr.*, **47**, 911–915.

Babin, M., Morel, A., Claustre, H., Bricaud, A., Kolber, Z. and Falkowski, P. G. (1996) Nitrogen- and irradiance-dependent variations of the maximum quantum yield of carbon fixation in eutrophic, mesotrophic and oligotrophic marine systems. *Deep-Sea Res. I*, **43**, 1241–1272.

Bidigare, R. R., Morrow, J. H. and Kiefer, D. A. (1988) Derivative analysis of spectral absorption by phytoplankton pigments. *Proceedings of SPIE (Ocean Optics IX)*, **925**, 101–108.

Bidigare, R. R., Morrow, J. H. and Kiefer, D. A. (1989) Derivative analysis of spectral absorption by photosynthetic pigments in the western Sargasso Sea. *J. Mar. Res.*, **47**, 323–341.

Bidigare, R. R., Ondrusek, M. E., Morrow, J. H. and Kiefer, J. H. (1990) *In vivo* absorption properties of algal pigments. *Proceedings of SPIE (Ocean Optics X)*, **1302**, 290–302.

Bissett, W. P., Patch, J. S., Carder, K. L. and Lee, Z. P. (1997) Pigment packaging and chlorophyll *a*-specific absorption in high-light oceanic waters. *Limnol. Oceanogr.*, **42**, 961–968.

Bouman, H. A., Platt, T., Kraay, G. W., Sathyendranath, S. and Irwin, B. D. (2000a) Bio-optical properties of the subtropical North Atlantic. 1. Vertical variability. *Mar. Ecol. Prog. Ser.*, **200**, 3–18.

Bouman, H. A., Platt, T., Sathyendranath, S., Irwin, B. D., Wernand, M. R. and Kraay, G. W. (2000b) Bio-optical properties of the subtropical North Atlantic. 2. Relevance to models of primary production. *Mar. Ecol. Prog. Ser.*, **20**, 19–34.

Bricaud, A. and Stramski, D. (1990) Spectral absorption coefficients of living phytoplankton and nonalgal biogenous matter: a comparison between the Peru upwelling area and the Sargasso Sea. *Limnol. Oceanogr.*, **35**, 562–582.

Bricaud, A., Morel, A. and Prieur, L. (1983) Optical efficiency factors of some phytoplankters. *Limnol. Oceanogr.*, **28**, 816–832.

Bricaud, A., Bédhomme, A.-L. and Morel, A. (1988) Optical properties of diverse phytoplanktonic species: experimental results and theoretical interpretation. *J. Plankton Res.*, **10**, 851–873.

Bricaud, A., Babin, M., Morel, A. and Claustre, H. (1995) Variability in the chlorophyll-specific absorption coefficients of natural phytoplankton: analysis and parameterization. *J. Geophys. Res.*, **100**, 13321.

Bricaud, A., Morel, A., Babin, M., Allali, K. and Claustre, H. (1998) Variations of light absorption by suspended particles with chlorophyll *a* concentration in oceanic (case 1) waters: analysis and implications for bio-optical models. *J. Geophys. Res.*, **103**, 31033–31044.

Bricaud, A., Allali, K., Morel, A., Marie, D., Veldhuis, M. J. W., Partensky, F. and Vaulot, D. (1999) Divinyl chlorophyll *a*-specific absorption coefficients and absorption efficiency factors for *Prochlorococcus marinus*: kinetics of photoacclimation. *Mar. Ecol. Prog. Ser.*, **188**, 21–32.

Campbell, L., Landry, M. R., Constantinou, J., Nolla, H. A., Brown, S. L., Liu, H. and Caron, D. A. (1998) Response of microbial community structure to environmental forcing in the Arabian Sea. *Deep-Sea Res. II, Topical Studies in Oceanography*, **45**, 2301–2325.

Carder, K. L., Chen, F. R., Lee, Z. P., Hawes, S. K. and Kamykowski, D. (1999) Semianalytic moderate-resolution imaging spectrometer algorithms for chlorophyll a and absorption with bio-optical domains

based on nitrate-depletion temperatures. *J. Geophys. Res.*, **104**, 5403–5421.

Carroll, C. L. (1999) *Size-fractionated Pigment Distribution in the Chesapeake Bay Outflow Plume*. Masters Thesis, The University of Southern Mississippi, Hattiesburg, MS.

Ciotti, A. M., Cullen, J. J. and Lewis, M. R. (1999) A semi-analytical model of the influence of phytoplankton community structure on the relationship between light attenuation and ocean color. *J. Geophys. Res. (C1)*, **104**, 1559–1578.

Ciotti, A. M., Lewis, M. R. and Cullen, J. J. (2002) Assessment of the relationships between dominant cell size in natural phytoplankton communities and the spectral shape of the absorption coefficient. *Limnol. Oceanogr.*, **47**, 404–417.

Cleveland, J. S. (1995) Regional models for phytoplankton absorption as a function of chlorophyll *a* concentration. *J. Geophys. Res.*, **100**, 13333–13344.

Cloutis, E. A. (1996) Hyperspectral geological remote sensing: evaluation of analytical techniques. *Int. J. Rem. Sens.*, **17**, 2215–2242.

DuRand, M. D., Olson, R. J. and Chisholm, S. W. (2001) Phytoplankton population dynamics at the Bermuda Atlantic Time-series station in the Sargasso Sea. *Deep-Sea Res. II, Topical Studies in Oceanography*, **48**, 1983–2003.

Duysens, L. N. M. (1956) The flattening of the absorption spectrum of suspensions as compared with that of solutions. *Biochim. Biophys. Acta*, **19**, 1–12.

Garver, S. A. and Siegel, D. A. (1997) Inherent optical property inversion of the ocean color spectra and its biogeochemical interpretation, 1, Time series from the Sargasso Sea. *J. Geophys. Res.*, **102**, 18607–18625.

Geider, R. J. and Osborne, B. A. (1987) Light absorption by a marine diatom: experimental observations and theoretical calculations of the package effect in a small *Thalassiosira* species. *Mar. Biol.*, **96**, 299–308.

He, M.-X., Liu, Z.-S., Du, K.-P., Li, L.-P., Chen, R., Carder, K. L. and Lee, Z.-P. (2000) Retrieval of chlorophyll from remote-sensing reflectance in the China Seas. *Appl. Opt.*, **39**, 2467–2474.

Hoepffner, N. and Sathyendranath, S. (1991) Effect of pigment composition on absorption properties of phytoplankton. *Mar. Ecol. Prog. Ser.*, **73**, 11–23.

Hoepffner, N. and Sathyendranath, S. (1993) Determination of the major groups of phytoplankton pigments from the absorption spectra of total particulate matter. *J. Geophys. Res.*, **98**, 22789–22803.

Johnsen, G., Nelson, N. B., Jovine, R. V. M. and Prèzelin, B. B. (1994) Chromoprotein- and pigment-dependent modeling of spectral light absorption in two dinoflagellates, *Prorocentrum minimum* and *Heterocapsa pygmaea*. *Mar. Ecol. Prog. Ser.*, **114**, 245–258.

Kirk, J. T. O. (1975) A theoretical analysis of the contribution of algal cells to the attenuation of light within natural waters 2. Spherical cells. *New Phytologist*, **75**, 21–36.

Kirk, J. T. O. (1994) *Light and Photosynthesis in Aquatic Ecosystems*, 2nd edn. Cambridge University Press, New York.

Lazzara, L., Bricaud, A. and Claustre, H. (1996) Spectral absorption and fluorescence excitation properties of phytoplanktonic populations at a mesotrophic and an oligotrophic site in the tropical North Atlantic (EUMELI program). *Deep-Sea Res. I*, **43**, 1215–1240.

Lohrenz, S. E. (2000) A novel theoretical approach to correct for pathlength amplification and variable sample loading in measurements of particulate spectral absorption by the quantitative filter technique. *J. Plankton Res.*, **22**, 639–657.

Lohrenz, S. E., Fahnenstiel, G. L., Kirkpatrick, G. J., Carroll, C. L. and Kelly, K. A. (1999) Microphotometric assessment of spectral absorption and its potential application for characterization of harmful algal species. *J. Phycol.*, **35**, 1438–1446.

Lohrenz, S. E., Redalje, D. G., Verity, P. G., Flagg, C. N. and Matulewski, K. M. (2002) Primary production on the continental shelf off Cape Hatteras, North Carolina. *Deep-Sea Res. II, Topical Studies in Oceanography* **49**, 4479–4509.

Lutz, V. A., Sathyendranath, S. and Head, E. J. H. (1996) Absorption coefficient of phytoplankton: regional variations in the North Atlantic. *Mar. Ecol. Prog. Ser.*, **135**, 197–213.

Mann, J. E. and Myers, J. (1968) On pigments, growth, and photosynthesis of *Phaeodactylum tricornutum*. *J. Phycol.*, **4**, 349–355.

Mitchell, B. G. (1990) Algorithms for determining the absorption coefficient of aquatic particulates using the quantitative filter technique (QFT). *Proceedings of SPIE (Ocean Optics* X), **1302**, 137–148.

Moore, L. R., Goericke, R. and Chisholm, S. W. (1995) Comparative physiology of *Synechococcus* and *Prochlorococcus*: influence of light and temperature on growth, pigments, fluorescence and absorptive properties. *Mar. Ecol. Prog. Ser.*, **116**, 259–275.

Morel, A. (1991) Light and marine photosynthesis: a spectral model with geochemical and climatological implications. *Prog. Oceanogr.*, **26**, 263–306.

Morel, A. and Bricaud, A. (1981) Theoretical results concerning light absorption in a discrete medium, and application to specific absorption of phytoplankton. *Deep-Sea Res. I*, **28**, 1375–1393.

Morel, A. and Bricaud, A. (1986) Inherent optical properties of algal cells including picoplankton: theoretical and experimental results. *Can. Bull. Fish. Aquat. Sci.*, **214**, 521–559.

Morel, A., Ahn, Y. H., Partensky, F., Vaulot, D. and Claustre, H. (1993) *Prochlorococcus* and *Synechococcus*: a comparative study of their optical properties in relation to their size and pigmentation. *J. Mar. Res.*, **51**, 617–649.

Nelson, N. B., Prezelin, B. B. and Bidigare, R. R. (1993) Phytoplankton light absorption and the package effect in California coastal waters. *Mar. Ecol. Prog. Ser.*, **94**, 217–227.

Platt, T. and Sathyendranath, S. (1988) Oceanic primary production: estimation by remote sensing at local and regional scales. *Science*, **241**, 1613–1620.

Roesler, C. S. and Perry, M. J. (1995) In situ phytoplankton absorption, fluorescence emission, and particulate backscattering spectra determined from reflectance. *J. Geophys. Res.*, **100**, 13279–13294.

Sakshaug, E., Bricaud, A., Dandonneau, Y., Falkowski, P. G., Kiefer, D. A., Legendre, L., Morel, A., Parslow, J. and Takahashi, M. (1997) Parameters of photosynthesis: definitions, theory and interpretation of results. *J. Plankton Res.*, **19**, 1637–1670.

Sathyendranath, S., Lazzara, L. and Prieur, L. (1987) Variations in the spectral values of specific absorption of phytoplankton. *Limnol. Oceanogr.*, **32**, 403–415.

Sathyendranath, S., Cota, G., Stuart, V., Maass, H. and Platt, T. (2001) Remote sensing of phytoplankton pigments: a comparison of empirical and theoretical approaches. *Int. J. Rem. Sens.*, **22**, 249–273.

Shalapyonok, A., Olson, R. J. and Shalapyonok, L. S. (2001) Arabian Sea phytoplankton during Southwest and Northeast Monsoons 1995: composition, size structure and biomass from individual cell properties measured by flow cytometry. *Deep-Sea Res. II, Topical Studies in Oceanography*, **48**, 1231–1261.

Sosik, H. M. (1996) Bio-optical modeling of primary production:

consequences of variability in quantum yield and specific absorption. *Mar. Ecol. Prog. Ser.*, **143**, 225–238.

Strain, H. H., Thomas, M. R. and Katz, J. J. (1963) Spectral absorption properties of ordinary and fully deuteriated chlorophylls *a* and *b*. *Biochim. Biophys. Acta*, **75**, 306–311.

Stuart, V., Sathyendranath, S., Platt, T., Maass, H. and Irwin, B. D. (1998) Pigments and species composition of natural phytoplankton populations: effect on the absorption spectra. *J. Plankton Res.*, **20**, 187–217.

Sunshine, J. M., Pieters, C. M. and Pratt, S. F. (1990) Deconvolution of mineral absorption bands: an improved approach. *J. Geophys. Res.*, **95**, 6955–6966.

Tassan, S. and Ferrari, G. M. (1995) An alternative approach to absorption measurements of aquatic particles retained on filters. *Limnol. Oceanogr.*, **40**, 1358–1368.

Tassan, S. and Ferrari, G. M. (1998) Measurement of light absorption by aquatic particles retained on filters: determination of the optical pathlength amplification by the 'transmittance-reflectance' method. *J. Plankton Res.*, **20**, 1699–1709.

Tassan, S., Ferrari, G. M., Bricaud, A. and Babin, M. (2000) Variability of the amplification factor of light absorption by filter-retained aquatic particles in the coastal environment. *J. Plankton Res.*, **22**, 659–668.

Trees, C. C., Clark, D. K., Bidigare, R. R., Ondrusek, M. E. and Mueller, J. L. (2000) Accessory pigments versus chlorophyll a concentrations within the euphotic zone: a ubiquitous relationship. *Limnol. Oceanogr.*, **45**, 1130–1143.

Ulloa, O., Sathyendranath, S. and Platt, T. (1994) Effect of the particle-size distribution on the backscattering ratio in seawater. *Appl. Opt.*, **33**, 7070–7077.

Wright, S. W., Jeffrey, S. W., Mantoura, R. F. C., Llewellyn, C. A., Bjornland, T., Repeta, D. and Welschmeyer, N. (1991) Improved HPLC method for the analysis of chlorophylls and carotenoids from marine phytoplankton. *Mar. Ecol. Prog. Ser.*, **77**, 183–196.

Received on April 28, 2002; accepted on September 1, 2002